Biochimica et Biophysica Acta 1837 (2014) 1395–1410

Contents lists available at ScienceDirect

Biochimica et Biophysica Acta

journal homepage: www.elsevier.com/locate/bbabio

Review

Water exchange in manganese-based water-oxidizing catalysts in photosynthetic systems: From the water-oxidizing complex in photosystem II to nano-sized manganese oxides ☆

Mohammad Mahdi Najafpour [a,b,*], Mohsen Abbasi Isaloo [a], Julian J. Eaton-Rye [c], Tatsuya Tomo [d], Hiroshi Nishihara [e], Kimiyuki Satoh [f,g], Robert Carpentier [h], Jian-Ren Shen [f,g], Suleyman I. Allakhverdiev [i,j,**]

[a] Department of Chemistry, Institute for Advanced Studies in Basic Sciences (IASBS), Zanjan 45137-66731, Iran
[b] Center of Climate Change and Global Warming, Institute for Advanced Studies in Basic Sciences (IASBS), Zanjan 45137-66731, Iran
[c] Department of Biochemistry, University of Otago, P.O. Box 56, Dunedin 9054, New Zealand
[d] Department of Biology, Faculty of Science, Tokyo University of Science, Kagurazaka 1-3, Shinjuku-ku, Tokyo 162-8601, Japan
[e] Department of Chemistry, School of Science, The University of Tokyo, 7-3-1 Hongo, Bunkyo-ku, Tokyo 113-0033, Japan
[f] Graduate School of Natural Science and Technology, Okayama University, Okayama 700-8530, Japan
[g] Faculty of Science, Okayama University, Okayama 700-8530, Japan
[h] Department de Chimie-Biologie, Université du Quebec à Trois Rivières, 3351, Boulevard des Forges, C.P. 500, Quebec G9A 5H7, Canada
[i] Institute of Plant Physiology, Russian Academy of Sciences, Botanicheskaya Street 35, Moscow 127276, Russia
[j] Institute of Basic Biological Problems, Russian Academy of Sciences, Pushchino, Moscow Region 142290, Russia

ARTICLE INFO

Article history:
Received 6 December 2013
Received in revised form 15 March 2014
Accepted 19 March 2014
Available online 29 March 2014

Keywords:
Artificial photosynthesis
Manganese
Nano-sized manganese oxide
Oxygenic photosynthesis
Photosystem II
Water exchange
Water-oxidizing complex

ABSTRACT

The water-oxidizing complex (WOC), also known as the oxygen-evolving complex (OEC), of photosystem II in oxygenic photosynthetic organisms efficiently catalyzes water oxidation. It is, therefore, responsible for the presence of oxygen in the Earth's atmosphere. The WOC is a manganese–calcium ($Mn_4CaO_5(H_2O)_4$) cluster housed in a protein complex. In this review, we focus on water exchange chemistry of metal hydrates and discuss the mechanisms and factors affecting this chemical process. Further, water exchange rates for both the biological cofactor and synthetic manganese water splitting are discussed. The importance of fully unveiling the water exchange mechanism to understand the chemistry of water oxidation is also emphasized here. This article is part of a Special Issue entitled: Photosynthesis Research for Sustainability: Keys to Produce Clean Energy.

1. Introduction

Oxygenic photosynthesis is a fundamental biological process by which cyanobacteria, algae, and plants reduce atmospheric CO_2 to energy-rich organic compounds using electrons extracted from water during water-splitting [1]. Photosynthetic water-splitting takes place in the water-oxidizing complex (WOC) of photosystem II (PSII), a large pigment-binding protein complex found in all oxygen-evolving organisms. To understand the mechanism of photoinduced water-splitting in PSII, a large number of studies have been carried out [1,2]. Pirson was the first to discover that Mn is essential for oxygenic photosynthesis [2,3] and extensive research since then has led to the establishment of the PSII pigment–protein complex to be responsible for photosynthetic oxygen evolution [4]. X-ray crystallographic analysis of thermophilic cyanobacterial PSII preparations has provided detailed information on the catalytic center of oxygen evolution [5–8].

The 1.9 Å resolution structural analysis (Fig. 1a) has revealed that the WOC contains five O atoms in addition to Mn_4Ca, forming a Mn_4CaO_5-cluster, and that they are arranged in a distorted chair-like form (Fig. 1a) [8]. In this chair form (Fig. 1a), three Mn (designated Mn1 to Mn3), one Ca, and four O atoms form a cubane-like structure, whereas the fourth Mn (Mn4) is located outside of the cubane and is associated with the cubic structure by μ-oxo-bridges (Fig. 1a). Four water molecules were found to serve as the terminal ligands to the metal cluster,

☆ This article is part of a Special Issue entitled: Photosynthesis Research for Sustainability: Keys to Produce Clean Energy.

* Correspondence to: M.M. Najafpour, Department of Chemistry, Institute for Advanced Studies in Basic Sciences (IASBS), Zanjan 45137-66731, Iran. Tel.: +98 241 415 3201; fax: +98 241 415 3232.
** Correspondence to: S.I. Allakhverdiev, Institute of Plant Physiology, Russian Academy of Sciences, Botanicheskaya Street 35, Moscow 127276, Russia. Tel.: +7 496 7731 837; fax: +7 496 7330 532.
E-mail addresses: mmnajafpour@iasbs.ac.ir (M.M. Najafpour), suleyman.allakhverdiev@gmail.com (S.I. Allakhverdiev).

http://dx.doi.org/10.1016/j.bbabio.2014.03.008
0005-2728/

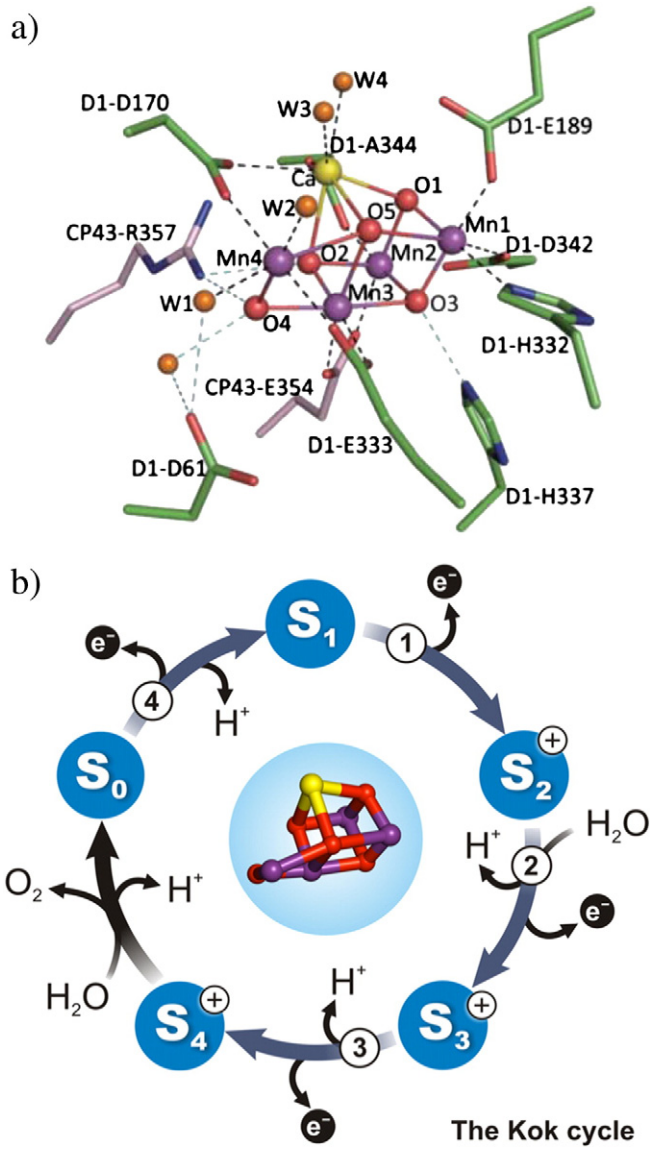

Fig. 1. There are only a small fraction of the residues that come in direct contact with the Mn–Ca cluster (image was modified from [8]) (a). Kinetic scheme (Kok cycle) describing the S_i state advancement by electron and proton removals from the WOC during water-splitting in PSII. Water-binding within the cycle is based on FTIR data by Noguchi [42,87]. Both waters likely represent ones that become substrates in the next cycle. Image is from [68] (b).

among which, two are ligated to Mn4 and the other two to the Ca ion. Some of these water molecules may serve as the substrate for water-splitting. For available kinetic, energetic, biochemical and structural information on the WOC see Refs. [9–11].

2. Flash-induced oxygen evolution pattern — the Joliot experiment and the Kok cycle

A first understanding of steps involved in oxygen evolution in photosynthesis became possible when short and intense light flashes, with appropriate dark periods, were used and oxygen evolution was measured per flash in a sequence of flashes. Experiments by Joliot in 1969 showed that flash illumination produced an oscillating pattern in the oxygen evolution and a maximum occurred on every *fourth* flash [12]. Water oxidation to produce one oxygen molecule requires the removal of four electrons, and Kok et al. [13] proposed an explanation for the observed oscillation of the oxygen evolution pattern. Kok's hypothesis was that in a cycle of water oxidation, a succession of oxidizing equivalents is stored at the WOC, and when four oxidizing equivalents have accumulated one by one, an oxygen molecule is spontaneously evolved [14]. Each oxidation state of the WOC is known as an "S-state", with S_0 being the most reduced state and S_4 the most oxidized state in the catalytic cycle (Fig. 1b) [13]. However, a tyrosine (Y_D) in PSII slowly oxidizes the WOC from S_0 to S_1 in the dark. States that are more reduced than S_0, such as S_{-1} and S_{-2}, are also possible [15].

In order to explain the fact that the first maximum of oxygen evolution is after the 3rd flash, and then after the 7th and the 11th flash, the S_1 state was concluded to be dark-stable. The $S_4 \rightarrow S_0$ transition is light independent and in this state oxygen is evolved. All other S-state transitions are initiated after photochemical oxidation of P_{680} at the PSII reaction center [13].

Even after the availability of 1.9 Å atomic structure of WOC [8], relatively little is known about the molecular mechanism of water oxidation. In this context, information on when the substrate water molecules bind to the catalytic site during the S_i state cycle of the photosynthetic oxygen evolution would be of significant value because it can provide a deeper insight into the mechanism of water oxidation. In addition, mimicking this reaction with synthetic analogs is expected to be of fundamental importance for bioinorganic chemistry of this system [16–31]. Additionally, Mn based water oxidation catalysts are important candidates for the development of artificial photosynthetic devices, i.e., systems for the synthesis of fuels such as hydrogen or methanol using solar energy [16–31]. In this review, we will focus on water exchange chemistry and explain different mechanisms and different factors in water exchange by metal ions. Then, we will consider water exchange for the Mn compounds as water-oxidizing catalysts in both artificial and natural photosynthetic systems.

3. Ion hydration/solvation

Many physico- and bio-chemical processes are directly controlled, or indirectly conditioned by metal ions [32]. In aqueous solution, metal ions are coordinated by water molecules, and, in addition to the first coordinated group, there are some water molecules in the second shell around the ions. The first solvation number, n, in $M(H_2O)_n$ of many metal ions has been determined directly by X-ray or neutron diffraction. Regarding the first shell, if $M(H_2O)_n$ exchanged water molecules rapidly (within a matter of seconds) it would be considered labile, whereas if it substituted slowly, it would be considered inert. The rate of exchange depends on the properties of the metal ion, the oxidation state, the ratio of the charge to the radius of metal ions and many other factors (Fig. 2) [13,33–35].

The water exchange is a substitution reaction. In a substitution reaction, also known as single displacement reaction or single replacement reaction, a group in a compound is replaced by another group [36,37]. For substitution reaction of metal complexes, Langford and Gray (1965) proposed three different mechanisms [38] (see Fig. 3 [39]):

a) A dissociative (D) reaction with an identifiable intermediate of low coordination number; it is called the D mechanism.
b) An associative (A) reaction with an identifiable intermediate of higher coordination number; it is called the A mechanism.
c) An interchange (I) reaction where the bond making and breaking were either synchronous or else took place within the pre-formed aggregate; it is called the I mechanism which is subdivided into dissociative-like (I_d) or associative-like (I_a) mechanism. Thus, the identification of an intermediate species is essential for the determination of the mechanism of reaction.

4. Activation parameters

By studying the effect of temperature or pressure on the water exchange rate, we expect to obtain useful information on the activation parameters of these reactions [35].

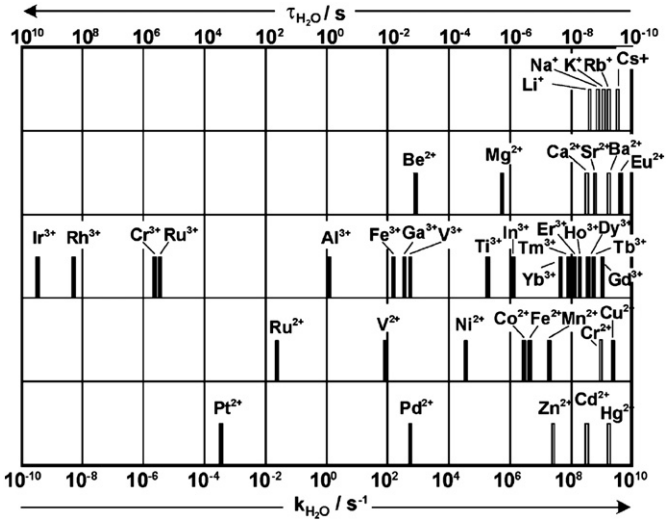

Fig. 2. Mean lifetimes, τ_{H2O}, of a particular water molecule in the first coordination shell of a given metal ion and the corresponding water exchange rate k_{ex} at 298 K. The filled bars indicate directly determined values, and the empty bars indicate values deduced from ligand substitution studies.
Image and caption from Ref. [34].

The effect of pressure on the rate constant of water exchange (k) at constant temperature for a reaction gives us the volume of activation [35]:

$$(\mathrm{dln}k/\mathrm{d}p)_T = -\Delta V^{\neq}/RT \quad (1)$$

where, p and T are the pressure and temperature, and $\Delta V^{\neq}$ is the volume of activation, k is the rate of exchange of water molecules, and R is the gas constant. Eq. (1) shows the partial molar volume change when the reactants are converted to the activated complex. Thus, usually a $\Delta V^{\neq} > 0$ shows D, or I_d, $\Delta V^{\neq} \sim 0$ shows I, and $\Delta V^{\neq} < 0$ shows A or I_a. Further, $\Delta H^{\neq}$ and $\Delta S^{\neq}$ refer to enthalpy (a measure of the total energy of reactant to activated complex) and entropy change when the reactants are converted to the activated complex.

Regarding, the three parameters, $\Delta V^{\neq}$, $\Delta H^{\neq}$ and $\Delta S^{\neq}$ especially $\Delta V^{\neq}$, we can find the mechanism for water exchange for metal compounds such as the Mn–Ca cluster in PSII.

The kinetic parameters for water exchange by several metal ions are shown in Tables 1–3.

The D mechanism is (Fig. 2):

$$M(H_2O)_6^{2+} \rightarrow M(H_2O)_5^{2+} + H_2O.$$

In other words, in this reaction, a water molecule will be separated from $M(H_2O)_6^{2+}$. Thus,

$$\Delta V^{'} = V\left(M(H_2O)_5^{2+}\right) + V(H_2O) - V\left(M(H_2O)_6^{2+}\right).$$

We know that $V(M(H_2O)_6^{2+}) > V(M(H_2O)_5^{2+})$ because $M(H_2O)_6^{2+}$ is a bigger molecule than $M(H_2O)_5^{2+}$, $\Delta V^{\neq} < V(H_2O)$. The volume of one mole of water molecules is 18 $cm^3\ mol^{-1}$. Thus, $\Delta V^{\neq} < 18\ cm^3\ mol^{-1}$.

In aqueous solution, $\Delta V^{\neq}$ will be near +9 to +11 $cm^3\ mol^{-1}$ for D mechanism, and −11 $cm^3\ mol^{-1}$ for A mechanism [35]. Thus, the designations I_a for V(II) and Mn(II), I for Fe(II), and I_d for Co(II) and Ni(II) are most appropriate for water exchange with these metal ions. As shown in Tables 1–3: more t_{2g} electron density, the less likely would be the associative path since the entering water molecules will be between the three-fold axes of the octahedral complex [35]. On the other hand, more electrons in e_g would increase instability of bond between metal and water molecules, and D or I_d mechanism is more favorable.

The negative signs of $\Delta V^{\neq}$ for $M(H_2O)_6^{3+}$ indicate an A mechanism for $Ti(H_2O)_6^{3+}$ and I_a for other $M(H_2O)_5(OH)^{2+}$ ions. It shows that the positive charges on metal causes an effect on interaction entering ligand and metal ion. Interestingly, a strong labilizing effect [40] is observed by deprotonation:

$$M(H_2O)_6^{3+} \rightarrow M(H_2O)_5(OH)^{2+} + H^+$$

that leads to a 10^2–10^3 fold enhanced rate for the hydroxy- over the hexaaqua ion (compare Table 2 with Table 3). We can observe again that the greater the t_{2g} electron density decreases the A mechanism shown by increasingly less negative Ti(III) to Fe(III).

The study of water exchange for terminal water coordinated to Mn(III) is also interesting. However, $Mn(H_2O)_6^{3+}$ is not stable because of disproportionation [41]:

$$Mn(III)(H_2O)_6^{3+} \rightarrow Mn(II)(H_2O)_6^{2+} + Mn(IV)O_2.$$

However, Mn(III) can be stabilized by some N-donor ligands [42]. Ivanović–Burmazovic's group studied the rate constants and the activation parameters for the water exchange process on Mn(III) porphyrins (Fig. 4a) using ^{17}O NMR techniques [43]. It is interesting to note that the water exchange rates for these complexes are very fast ($1.0–2.5 \times 10^7$) almost identical to the rate in the case of $[Mn(H_2O)_6]^{2+}$.

Ivanović–Burmazovic's group proposed that Jahn–Teller distortion in the d^4 high-spin electronic configuration of Mn(III) and the cis-effect of porphyrin ligands are important factors for the fast water exchange of these complexes. Moderated to small values of $\Delta H^{\#}$ and $\Delta S^{\#}$ show that an interchange water exchange mechanism is operative under this condition independent of the complex charge and the nature of the axial ligand. The volume of activation offers clearer mechanistic insights, and its small positive values suggest that substitution of coordinated water follows a dissociative interchange (I_d) rather than a pure interchange (I) mechanism. Ivanović–Burmazovic's group suggested [43] that the fast water exchange is also observed for the four waters of the WOC because most probably carboxylate instead of porphyrin groups induces labialization for metal ions [44–47]. On the other hand, OH and μ-O also enhance the reactivity of the bound waters [48].

5. Two and multinuclear metal complexes

The Spiccia group has studied the kinetics of water exchange in Cr complexes, such as $[(H_2O)_4Cr(\mu\text{-}OH)_2Cr(H_2O)_4]^{4+}$, using ^{18}O labeling at 298 K see [49]. Data shows that there are two rate constants ($k_{trans} = 3.6 \times 10^{-4}\ s^{-1}$ and $k_{cis} = 6.6 \times 10^{-5}\ s^{-1}$) corresponding to the exchange of coordinated water molecules occupying trans and cis positions to the bridging OH groups.

A correlation between exchange rates for OH/Cr ratio for both bridging and terminal hydroxide groups was observed. The rates of water exchange on fully protonated dimer (OH/Cr = 1) are 28 and 150 times faster than exchange on Cr(III) (OH/Cr = 0) for waters cis and trans to the hydroxide bridges, respectively, as discussed by Leone Spiccia's group [49]. The two corresponding rates of exchange are 27 and 70 times faster on mono-deprotonated dimer (OH/Cr = 1.5) than on $[CrOH]^{2+}$. Spiccia's group suggested that the degree of condensation of the oligomer is one important factor, which will determine the rates of water exchange on that oligomer. The rates of water exchange on the Cr(III) dimer are in fact very similar to that reported for $Cr(H_2O)_5OH^{2+}$ (OH/Cr = 1) for both monomer and dimer, and much faster than the rate of exchange on $Cr(H_2O)_6^{3+}$. Thus, the bridging OH groups are comparable to terminal OH group in terms of their effect on the rate of substitution at Cr(III) [49].

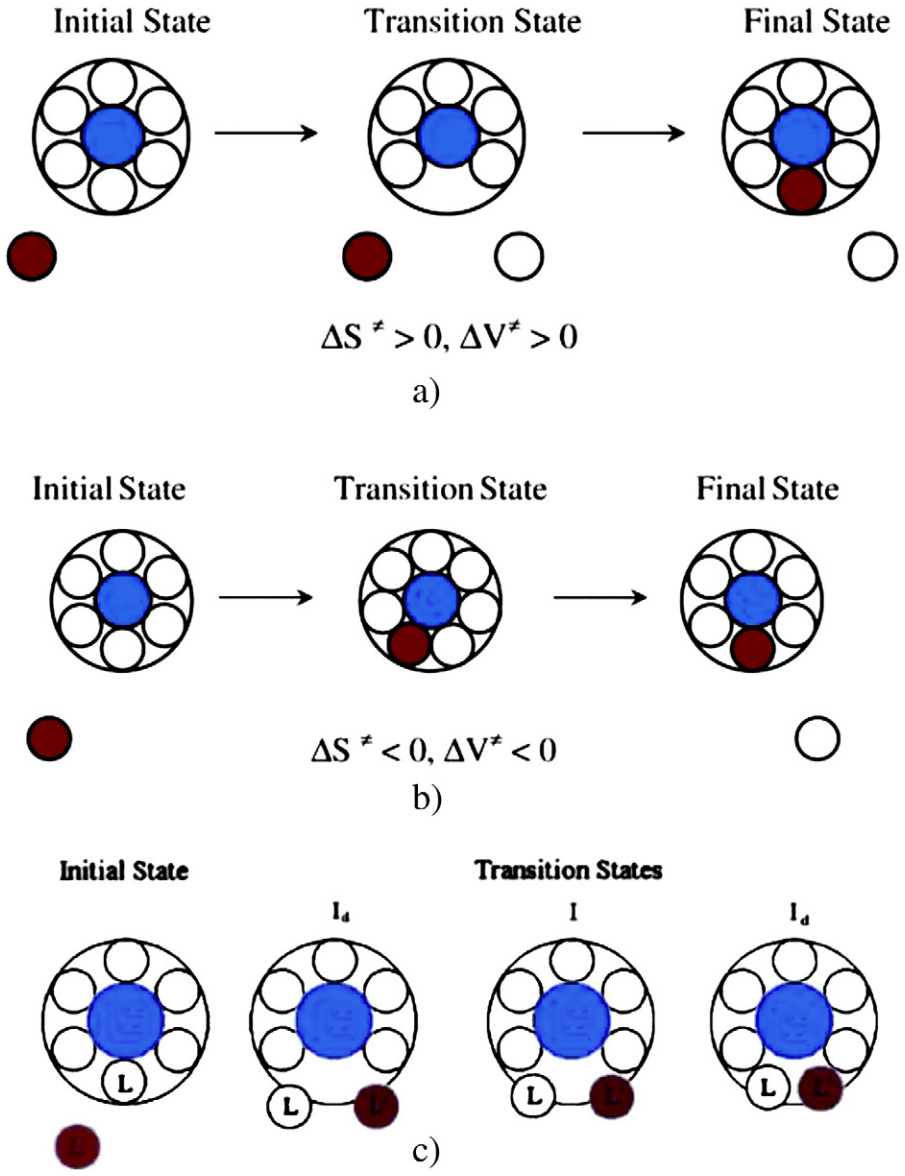

Fig. 3. Schematic representation of ligand exchange reactions proceeding by dissociative (D) mechanism (a), by associative (A) mechanism (b), and by interchange (I) mechanisms (c). The blue circle in the middle of the idealized 'flat' complex represents the central ion. The small open circles represent the bound ligands. The red circle represents the incoming ligand. The large circles enclosing the small ones represent the boundaries of the first coordination sphere.
Images and captions from [39].

Interestingly, inert Cr(III) and Cr(III) oligomers, by more condensation, convert into relatively labile ions. For example, exchange rates of about 0.1, 100, and 10^4 s^{-1} can be interpolated for ions with OH/Cr ratios of 2, 3, and 4, respectively.

The rates of isotopic oxygen exchange for $[Mo_3O_4(OH)_9]^{4+}$ (Fig. 4b) were reported by Rodgers' group. For the oxygens of type B and bridging oxygens, the rate was much too slow to follow to any major extent (Table 4) [50].

From these data, Rodgers' group concluded that there was a natural slowness of bridging oxygens (types A and B) in exchanging with the solvent. Rodgers' group also suggested that the metal–metal interaction most likely renders associative interactions energetically unfavorable.

In 1998, Van Eldik and his co-workers published high-pressure ^{17}O NMR studies on the dihydroxo-bridged rhodium(III) hydrolytic dimer (see e.g., Fig. 4c) [51]. They found that the introduction of bridging OH groups in the dimer labilized the bound waters but not to the same

Table 1
Kinetic parameters for water exchange of divalent transition metal ions, $M(H_2O)_6^{2+}$ at 25 °C [17].

Parameter	V(II)	Mn(II)	Fe(II)	Co(II)	Ni(II)
K (s^{-1})	89	2.1×10^7	4.4×10^6	3.2×10^6	3.2×10^4
$\Delta H^{\neq}$ (kJ mol^{-1})	62	33	41	47	57
$\Delta S^{\neq}$ ($J \cdot K^{-1} \cdot mol^{-1}$)	−0.4	+6	+21	+37	+32
$\Delta V^{\neq}$ (cm^3 mol^{-1})	−4.1	−5.4	+3.8	+6.1	+7.2
Electronic configuration	$(t_{2g})^3(e_g)^0$	$(t_{2g})^3(e_g)^2$	$(t_{2g})^4(e_g)^2$	$(t_{2g})^5(e_g)^2$	$(t_{2g})^6(e_g)^2$

Table 2
Kinetic parameters for water exchange of trivalent transition metal ions, $M(H_2O)_6^{3+}$ at 25 °C [17].

Parameter	Ti(III)	V(III)	Cr(III)	Fe(III)
k (s^{-1})	1.8×10^5	5.0×10^2	2.4×10^{-6}	1.6×10^2
$\Delta H^{\neq}$ (kJ mol^{-1})	43	49	109	64
$\Delta S^{\neq}$ ($J \cdot K^{-1} \cdot mol^{-1}$)	+1	−28	+12	+12
$\Delta V^{\neq}$ (cm^3 mol^{-1})	−12.1	−8.9	−9.6	−5.4
Electronic configuration	$(t_{2g})^1(e_g)^0$	$(t_{2g})^2(e_g)^0$	$(t_{2g})^3(e_g)^0$	$(t_{2g})^3(e_g)^2$

extent as deprotonation of the monomer did. The kinetic results suggested a limiting dissociative pathway (D) for water exchange in both the cis and trans positions in this system.

6. Mn-based metal complexes

Cooper et al. found that μ-O exchange occurred only at elevated temperatures for $[L_2MnO_2MnL_2]^{3+}$, where L = 2,2′-bipyridine (bpy) or 1,10-phenanthroline (phen) [17]. The isotopic exchange between oxygens of water and μ-O bridges in the di-μ-O diMn complexes, $[(mes\text{-}terpy)_2Mn_2^{III/IV}(\mu\text{-}O)_2(H_2O)_2](NO_3)_3$ (4′-mesityl-2,2′:6′,2″-terpyridine) (mes-terpy) and $[(phen)_4Mn_2^{III/IV}(\mu\text{-}O)_2](ClO_4)_3$ (Fig. 5), was investigated by considering the kinetics of exchange [52]. In this method, the isotope patterns from the mass spectra due to a given chemical species are altered upon isotope exchange. In other words, heavier isotopes were incorporated in place of lighter ones, thus it is observed that the peak at the lowest mass in the isotope pattern decreases in intensity, and the isotope pattern increases to higher masses. Crabtree and Brudvig, regarding isotope pattern at any time, showed a superposition of the isotope patterns due to unexchanged and exchanged species [52]. The signal intensities due to unexchanged and exchanged species are deconvoluted from each spectrum and normalized against total intensity to obtain concentrations of unexchanged and exchanged species, as explained below [52].

The results show that the presence of terminal water-binding sites in mes-terpy is a very important factor in water exchange in this complex. As shown by Crabtree and Brudvig's groups, the dependence of initial rates of μ-O exchange on $[H_2^{18}O]$ has a nearly linear and a nonlinear saturation behavior in the same concentration range for mes-terpy and phen, respectively [52]. These results show that water exchange for both complexes occurs in at least one step, which affects the overall rate of exchange. It is interesting that as the group indicated that the exchange rates increased for mes-terpy with the addition of acid but decreased for phen, indicating that the mechanisms of exchange in mes-terpy and phen are different. On the other hand, free ligand had no effect on the exchange rate for mes-terpy but decreased the exchange rate for phen. Crabtree and Brudvig's groups proposed four steps for water exchange for mes-terpy [52]:

(1) Two protonations of the bridging oxygen.
(2) Two deprotonations of the labeled water molecule.
(3) The breaking of two bonds between the bridging oxygen and the two Mn ions being bridged.
(4) The formation of two bonds between the oxygen of labeled water and the two Mn ions to be bridged.

Table 3
Kinetic parameters for water exchange of trivalent transition metal ions, $M(H_2O)_5OH^{2+}$ at 25 °C [17].

Parameter	$Cr(H_2O)_5OH^{2+}$	$Fe(H_2O)_5OH^{2+}$
k (s^{-1})	1.8×10^{-4}	1.2×10^5
$\Delta H^{\neq}$ (kJ mol^{-1})	110	42
$\Delta S^{\neq}$ ($J \cdot K^{-1} \cdot mol^{-1}$)	+55	+5
$\Delta V^{\neq}$ (cm^3 mol^{-1})	+2.7	+7.0
Electronic configuration	$(t_{2g})^3(e_g)^0$	$(t_{2g})^3(e_g)^2$

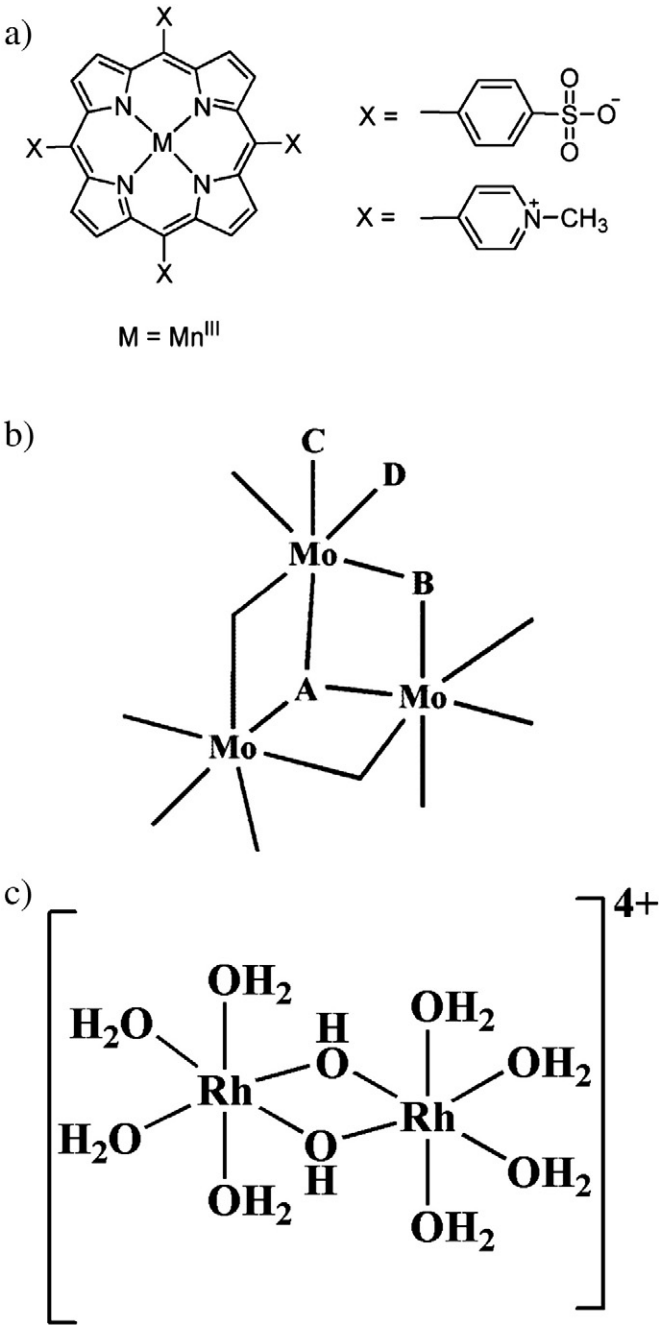

Fig. 4. Mn(III) porphyrins studied for water exchange (a). The structure of $[Mo_3O_4(OH)_9]^{4+}$ (b). The structure of dihydroxo-bridged rhodium(III) hydrolytic dimer (c).

The bridge-opening step has been proposed as either associative [53] or dissociative [54] (Fig. 6).

The temperature-dependence experiment for mes-terpy yields a large negative entropy of activation, favoring an associative mechanism ($\Delta S^{\#}$ and $\Delta H^{\#}$ are -151 $J \cdot K^{-1} \cdot mol^{-1}$ and 39, respectively) [52].

Table 4
$\tau_{1/2}$ for the exchange of different O atoms in $[Mo_3O_4(OH)_9]^{4+}$ shown in Fig. 4.

Oxygen type	Protons	Mo–O	$\tau_{1/2}$ (temperature °C)
A	0	2.020 (3)	10^5 (0)
B	0	1.916 (7)	2×10^8 (22)
C	2	2.163 (3)	2×10^5 (0)
D	2	2.26 (2)	10^3 (0)

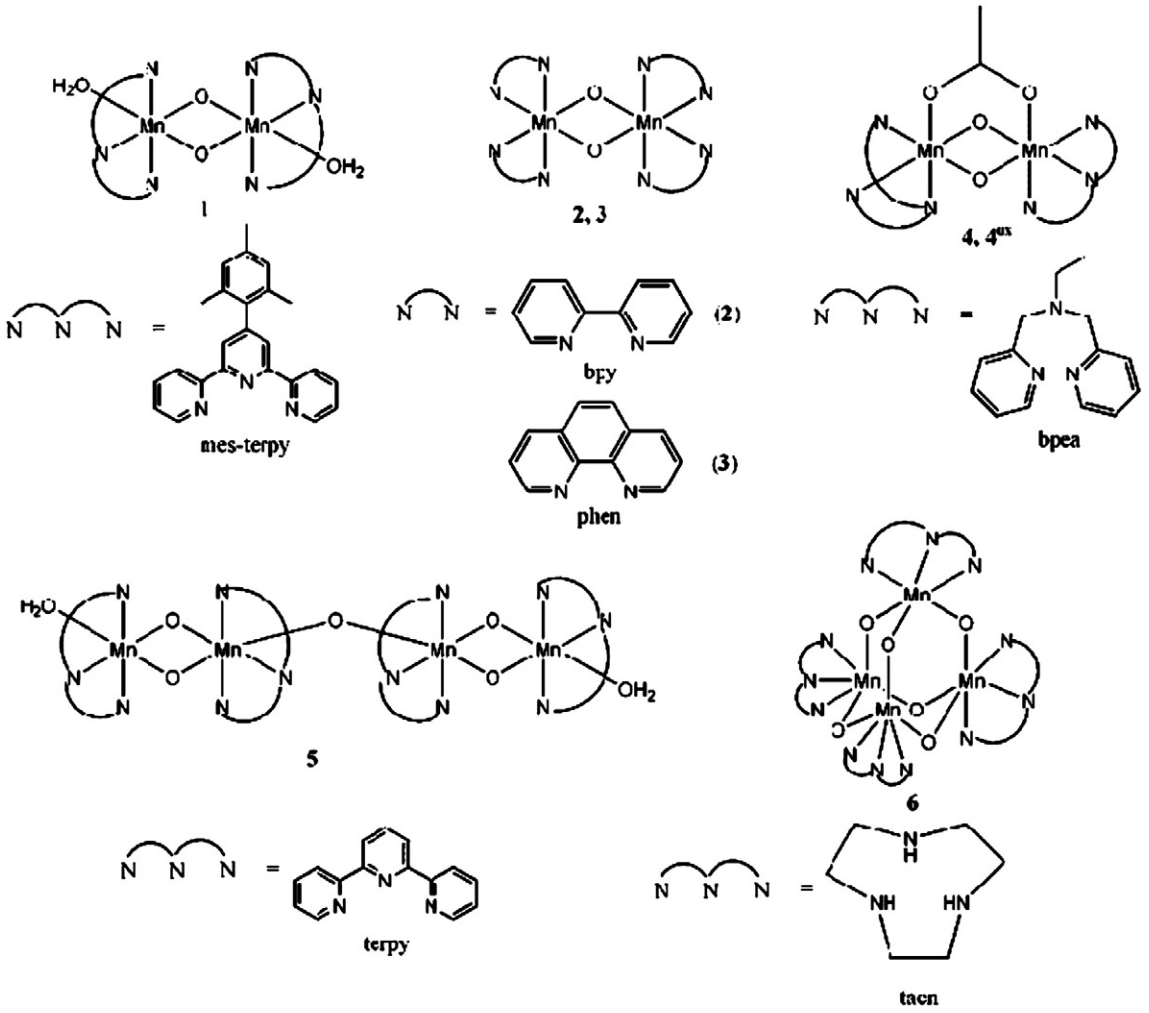

Fig. 5. Different multinuclear Mn complexes that their μ-O and μ-OAc exchange processes were considered by Crabtree and Brudvig's groups. Image from Ref. [52].

The proposed mechanism for water exchange by phen is shown in Fig. 7. In this mechanism a loss of phen is important and provides explanation for the following (see Ref. [52]):

- The slow rate of μ-O exchange as compared to mes-terpy.
- Inhibition of exchange by added phen ligand.
- Inhibition of exchange by stoichiometric amounts of acid.

The group concluded that [52]:

- Water exchange for Mn(IV) oxidation state is much slower than those which can switch between Mn(IV) and (III) states.
- The availability of terminal water-binding sites on Mn enhances μ-O exchange rates.
- It is very unlikely that the fast isotope exchange rates measured in the WOC (800–4000 times greater than those in mes-terpy) are μ-O exchange rates.

However, the μ-O exchange rate for mes-terpy up to a concentration of 7.4 M $H_2^{18}O$ gives a rate of $7.5 \times 10^{-2}\ s^{-1}$ that is similar to the slowest exchange rate measured in the WOC (2.2×10^{-2}) for the slow exchange rate in the S_1 state. It is important to note that the number is much smaller than the fast exchange rates in all states and the slow exchange rates in the S_0, S_2, and S_3 states.

- Half-lives for dimeric Mn (III, IV) are between 5 min and half an hour at 20 °C. Mn catalase in its Mn(III)–Mn(IV) state has an even longer time for the exchange [55].

In addition to mes-terpy and phen, Crabtree and Brudvig groups considered μ-O and μ-OAc exchange processes for other complexes (Fig. 5) [52]. The results are shown in Table 5.

In 2009, Spiccia and Casey's groups considered water exchange for a tetranuclear Mn cluster, $[Mn_4O_4L_6]$, where $L = [O_2P(C_6H_4OCH_3)_2]^-$, that has a "$Mn_4O_4$ cubane" core (Fig. 8) [56].

They added 10–40 μL $H_2^{18}O$ to a 0.125–0.500 mM solution of $[Mn_4O_4L_6][ClO_4]$, in 4 mL acetonitrile, and then following the incorporation of ^{18}O into $[Mn_4O_4L_6]^+$ by electrospray ionization mass spectroscopy (ESI-MS). They also studied effects of temperature, water concentration, concentration of $[Mn_4O_4L_6][ClO_4]$ and the presence of different acids [56]. Analysis of the temperature dependence of the oxygen exchange from 20 to 60 °C yield shows $\Delta S^{\#}$ and $\Delta H^{\#}$ of $-135 \pm 22\ J \cdot K^{-1} \cdot mol^{-1}$ and 59 ± 7 kJ mol^{-1}, respectively, for k_A [56]. The negative value of $\Delta S^{\#}$ indicates that the rate-limiting step for oxygen exchange in this tetranuclear Mn_4O_4 cluster is associative. They proposed that the reaction involves binding of a water molecule with a Mn site on the cluster followed by a cascade of bridge formation and cleavage processes that ultimately result in μ_3-O bridge exchange. They indicated that the μ_3-oxo groups in the $[Mn_4O_4L_6]^+$ cluster generally react with water on a timescale on the order of ca. ten-hour half-life at 20 °C [56].

In 2013, Agapie has synthesized cuboidal Mn_3CaO_3 or Mn_3CaO_4 complexes as models for the WOC in PSII (Fig. 9) [57].

$Mn(IV)_3CaO_4$ showed no oxygen atom transfer to tri-methylphosphine but the $Mn(III)_2Mn(IV)_2O_4$ cubane reacts with tri-methylphosphine within minutes to generate a novel $Mn(III)_4O_3$ partial cubane and

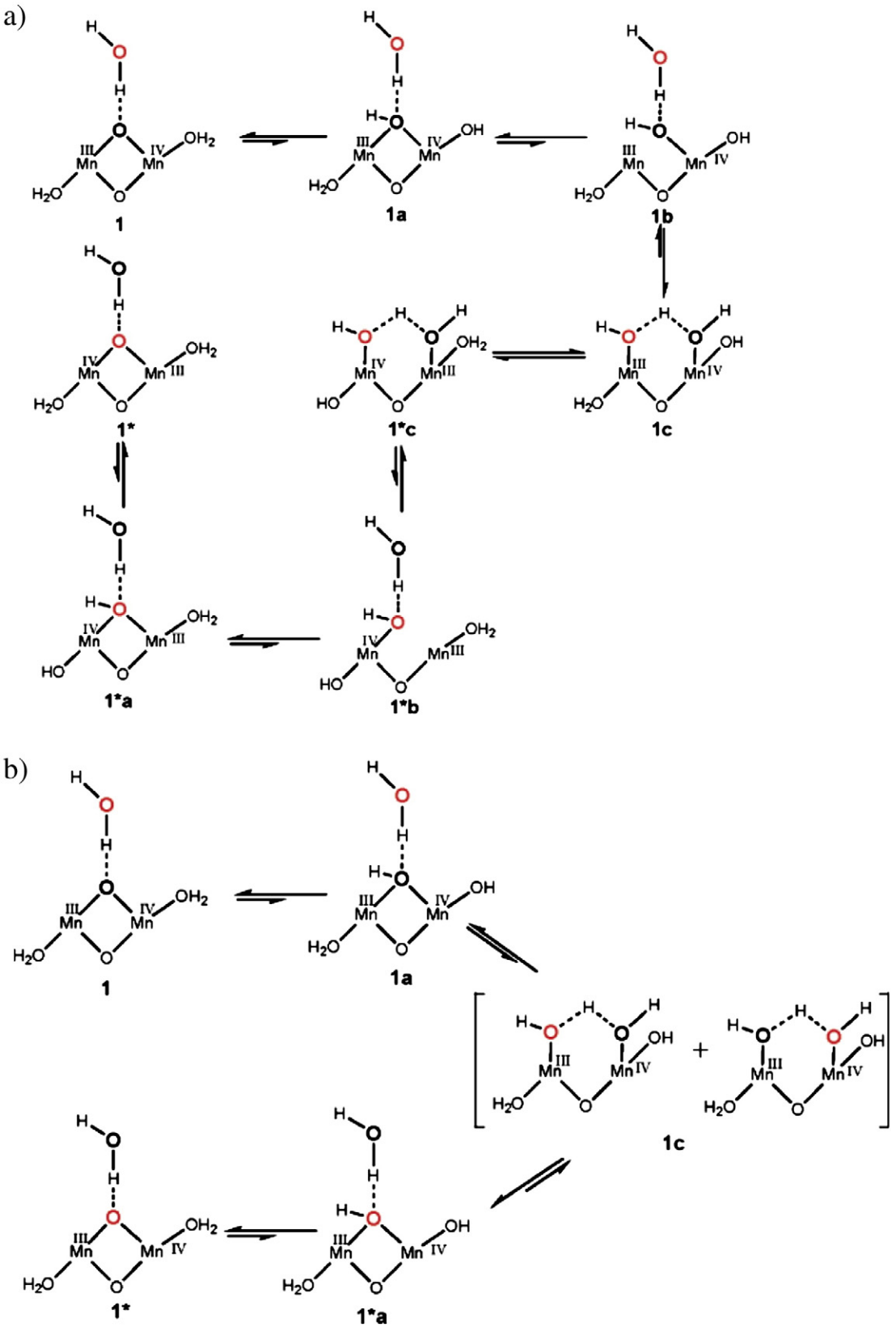

Fig. 6. Proposed dissociative mechanism of μ-O exchange in 1, involving sequential oxo-bridge opening and labeled water coordination (a). Proposed associative mechanism of μ-O exchange in 1, involving concerted oxo-bridge opening and labeled water coordination (b).
Images and captions from [28].

trimethylphosphine oxide. Using quantum mechanics (QM) for the oxygen transfer reaction from $Mn(III)_2Mn(IV)_2O_4$ and $Mn(IV)_3CaO_4$, they found that the preferred mechanism involves CH_3COO^- ligand dissociation and coordination with PMe_3 [57]. This reaction leads to a five-coordinated phosphorus (P) transition state that is 5–10 kcal/mol lower than when all CH_3COO^- ligands are attached. This dissociation

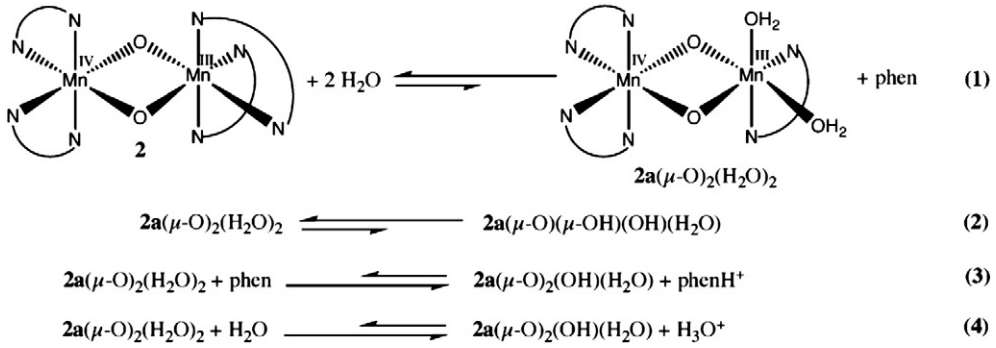

Fig. 7. Ligand dissociation and water coordination 2 proposed as requirements for μ-O exchange. Image and caption from [28].

of the CH_3COO^- ligand occurs only when Mn(III) is present. Experimentally, the rate of exchange between metal-bound acetates and CD_3COO^- was highest for $Mn(III)_2Mn(IV)_2O_4$, in agreement with the calculations [57]. These results indicate that even with a strong oxygen atom acceptor, such as tri-methylphosphine, the oxygen atom transfer chemistry from Mn_3CaO_4 cubanes is controlled by ligand lability, with the $Mn(IV)_3CaO_4$ WOC model being unreactive. The group isolated $Mn(III)_4O_3$ partial cubane upon oxygen atom transfer, without over reduction. The group also considered ^{18}O-labeling experiments via two-step conversions, from $Mn(III)_4O_3$ to $Mn(III)_2Mn(IV)_2O_4$ (with $H_2^{18}O$) and back to $Mn(III)_4O_3$ (with phosphine). These results insight into this two electron, two-proton process with respect to the position of incorporation into the partial cubane structure and support reaction mechanisms involving migration of oxide moieties within the cluster and are not consistent with selective oxide incorporation at the site available in the starting species, thus supporting the possibility of such migration processes during water incorporation into the WOC during turnover [57].

7. Water-oxidizing complex in photosystem II

In 2011, the research groups of Shen and Kamiya reported the structure of WOC with high resolution (Fig. 1) [8].

Their structure has provided many more details concerning the number and location of the bridged oxygens, the location of putative substrate water molecules and the precise arrangement of the amino-acid side chains [8]. In the structure [8], four Mn and one Ca ions, and five oxygen atoms form a $Mn_4CaO_5(H_2O)_4$ cluster. However, mechanism of water oxidation and O_2 production by the enzyme is still unclear. The substrates are important for understanding the mechanism of O–O bond formation, and one or two of four water molecules in addition to oxygen bridges in the cluster are proposed as substrate for O_2.

Water exchange measurements have been used to probe the binding of the substrate water at the WOC in PSII. Wydrzynski's group [33] used $H_2^{18}O$ exchange kinetics to examine the interactions of Ca and Sr with substrate water and to probe a number of point mutations surrounding

Table 5
Observed rate constants obtained at 20 °C for μ-O and μ-OAc exchange processes. [Mn-complexes] = 600 μM, [$H_2^{18}O$] = 260 mM, ([CD_3COOD]) 550 μM. Rates measured in solutions containing both 4 and 4^{ox} (oxidized form from 4) represent the lower limit and upper limit, respectively, for exchange processes in 4 and 4^{ox}, to account for the possibility of interconversion between 4 and 4^{ox}. Data and caption are from Ref. [33,36]. The numbers 1–6 (including 4^{ox}) correspond to the structure shown in Fig. 5.

Reactant	Ligand exchanged	k_{obs} (s^{-1}), $\tau_{1/2}$ (s)	Oxidation state of Mn
1 + $H_2^{18}O$	μ-O	$(2.5 \pm 0.2) \times 10^{-3}$, 280 ± 20	(III, IV)
2 + $H_2^{18}O$	μ-O	$(5.4 \pm 0.2) \times 10^{-4}$, 1280 ± 50	(III, IV)
3 + $H_2^{18}O$	μ-O	$(6 \pm 1) \times 10^{-4}$, 1200 ± 200	(III, IV)
4 + $H_2^{18}O$	μ-O	$(4.5 \pm 0.2) \times 10^{-4}$, 1540 ± 70	(III, IV)
4^{ox} + $H_2^{18}O$	μ-O	$(5.0 \pm 0.3) \times 10^{-5}$, 13,900 ± 800	(IV, IV)
4 + CD_3COOD	μ-OAc	$\geq 5.5 \times 10^{-2}$, ≤13	(III, IV)
4^{ox} + CD_3COOD	μ-OAc	$(1.6 \pm 0.1) \times 10^{-4}$, 4300 ± 300	(IV, IV)
5 + $H_2^{18}O$	μ-O	$\leq 2 \times 10^{-7}$, $\geq 3 \times 10^6$	(IV, IV, IV, IV)
6 + $H_2^{18}O$	μ-O	$\leq 1 \times 10^{-8}$, $\geq 6 \times 10^7$	(IV, IV, IV, IV)

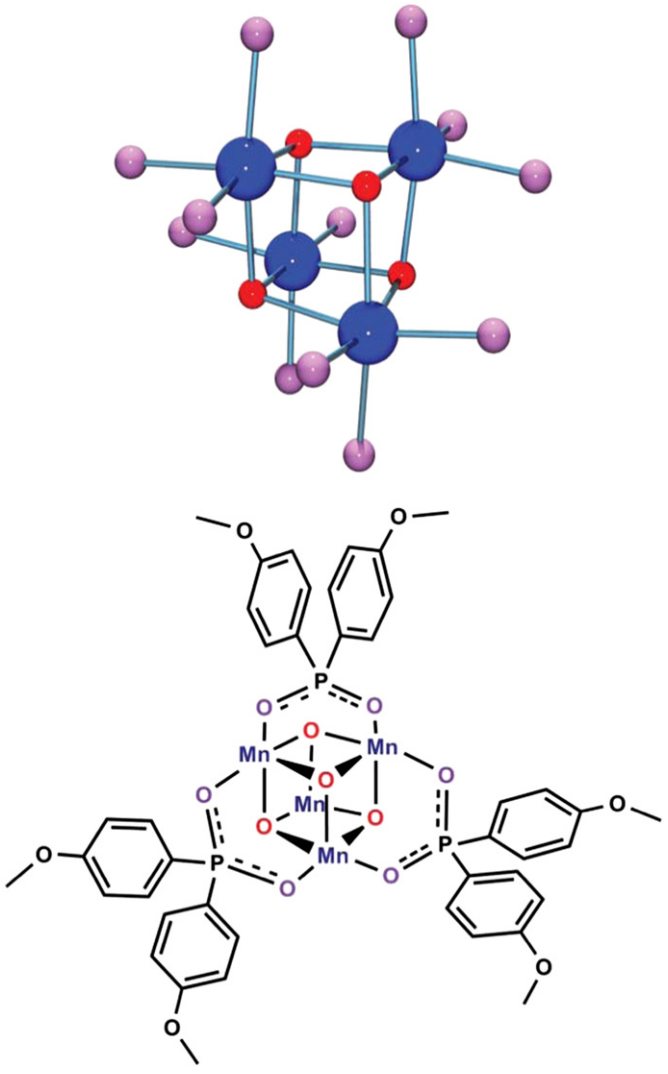

Fig. 8. Structure of the Mn_4O_4 cubane core (top) and schematic structure showing three of the six ligands (bottom). Mn ions in blue, inert phosphinate oxygen atoms in violet and exchanging oxygen atoms in red.
Image and caption from [56].

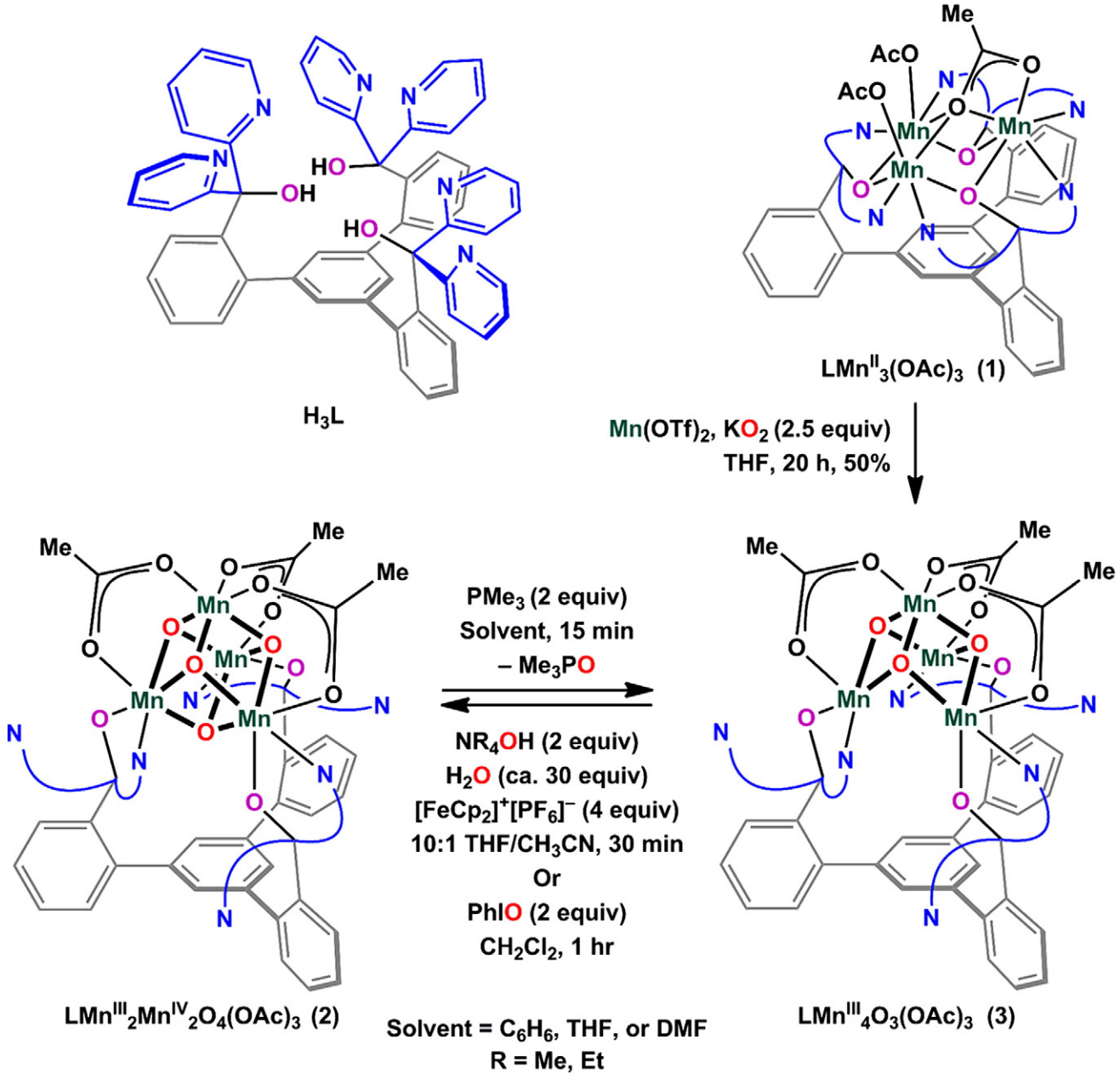

Fig. 9. The structure and procedure method to synthesis of Mn–Ca complex.
Image and caption from Ref. [57].

the catalytic site by MIMS [58,59]. The MIMS method involves the addition of ^{18}O water followed by time dependent sampling of the products. In this technique, two kinetic phases at m/e = 34, representing separate ^{18}O exchange rates for the two substrate water molecules, were detected [33]. The slow and fast phases demonstrate that the two substrate water molecules bind at two chemically distinct, no equivalent sites. In addition to four water molecules found in the WOC, μ-O groups and water molecules around the WOC are proposed as a substrate for water oxidation. The results show that the slow site in S_0 exchange is more tightly bound in S_1 by (500 times) regarding Mn oxidation [33]. However, the slow site is less tightly bound in S_2 (100 times) and remains unchanged in the S_3 state (Table 6).

If we consider the results for Mn ions in the Mn–Ca cluster in PSII, we may suggest that the rate of water exchange in the cluster should be faster than mononuclear metal ions because:

a) The cluster is a delocalized system and charge on each Mn ion is less than a separated Mn ion. Thus, the rate of water exchange is most probably faster in a cluster than with separated ions.
b) Regarding the 10^2–10^3 fold enhanced rate for the hydroxy- over the hexaaqua ion, most probably the cluster with μ-O group provides higher rates of water exchange as shown by some groups and in

Table 6
S_i state dependence of substrate water exchange rates measured by MIMS in spinach thylakoids with Ca and Sr-substituted BBY [11].

S_i	k_s (Ca) (s^{-1})	k_f (Ca) (s^{-1})	k_s (Sr) (s^{-1})	k_f (Sr) (s^{-1})
S_0	~10	>120	–	–
S_1	~0.02	>120	~0.08	>120
S_2	~2.0	~120	~9.0	>120
S_3	~2.0	~40	~6.0	~23

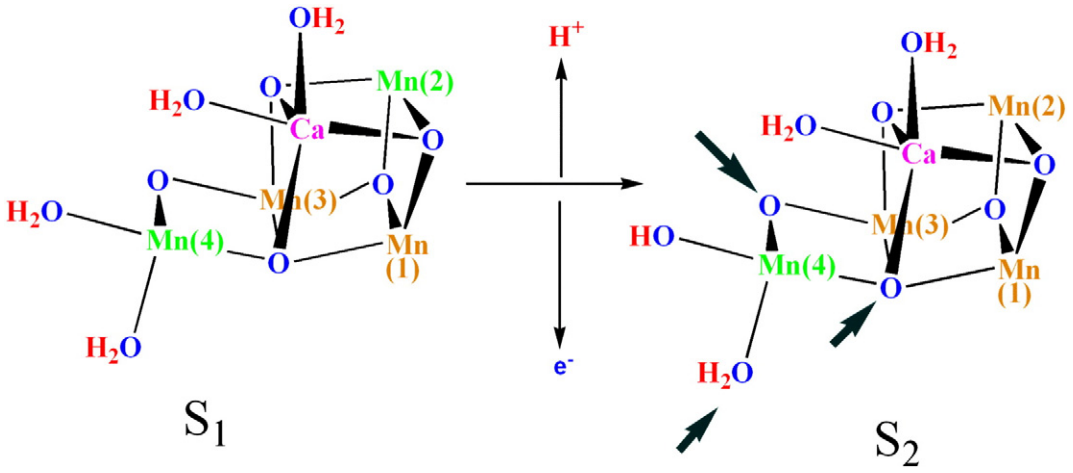

Fig. 10. A proposed mechanism for S_1 to S_2 state transitions. Orange and green Mn ions are Mn(IV) and Mn(III), respectively. Regarding our hypothesis, deprotonation for a coordinated water molecule to Mn ion, increases water exchange for the oxygen shown with black arrows.

different complexes as we discussed in previous sections. The increased rate of water exchange in S_1 to S_2 can be related to a deprotonation in two nearby water molecules. This can be due to two coordinated water molecules or μ-OH groups to a Mn ion during S_1 to S_2 transition, one of them being deprotonated. In the transition state, the oxidation occurs for another Mn ion (Fig. 10). The intrinsic proton releasing pattern from the WOC in the S transitions ($S_0 \rightarrow S_1$, $S_1 \rightarrow S_2$, $S_2 \rightarrow S_3$, and $S_3 \rightarrow [S_4] \rightarrow S_0$) appears to be 1, 1, 1, 1 in spinach PSII core preparations and around 1, 0, 1, 2 in preparations that include more protein subunits [60,61]. If we accept 1, 0, 1, 2 pattern for proton releasing, then the S_1 to S_2 transition may implicate an intra-molecular proton transfer between the μ-O or water molecules in the Mn–Ca cluster.

c) The mechanism of water exchange for the Mn ions in the WOC is most probably D or I_d substitution reaction because each Mn ion in the structure is coordinated to at least one O or OH groups.

Thus, it is likely that the oxidation number of a Mn ion changes but deprotonation occurs for a water molecule coordinated to another Mn ion. From the summarized data, we suggest a high rate of water exchange for $Mn(H_2O)_6^{3+}$ above 1.6×10^2 observed for $Fe(H_2O)_6^{3+}$ because of a Jahn–Teller effect. As we discussed before, rates of $1.0–2.5 \times 10^7$ were reported for Mn(III) porphyrin and rates faster than 1.2×10^5 were observed for $Mn(H_2O)_5(OH)^{2+}$. However, a very slow rate is suggested for $Mn(H_2O)_6^{4+}$, but it is important to note that this ion is strongly acidic, and hydrolyzes to:

$$Mn(H_2O)_6{}^{4+} \rightarrow Mn(H_2O)_5(OH)^{3+} + H^+$$

$$Mn(H_2O)_5(OH)^{3+} \rightarrow Mn(H_2O)_4(OH)_2{}^{2+} + H^+$$

$$Mn(H_2O)_5(OH)_2{}^{2+} \rightarrow Mn(H_2O)_4(OH)_3{}^{+} + H^+.$$

We may assume rates less than 2.4×10^{-9} s^{-1} for $Mn(H_2O)_6^{4+}$ with $(t_{2g})^3$ electronic configuration similar to Cr(III), but it is more positive than $Cr(H_2O)_6^{3+}$. However, considering the three deprotonation steps for $Mn(H_2O)_6^{4+}$ ($10^3 \times 10^3 \times 10^3$), the rate will be ~1 for $Mn(H_2O)_3(OH)_3^{+}$. Hence, a rate of 0.02–2 for Mn(IV)–O is possible. On the other hand, other ligands in the compound may increase the rate of water exchange. For example, rates of ~10^2 s^{-1} were postulated, for both water exchange and intramolecular OH-bridge formation, for ions with a OH^-/Cr(III) ratio of 3 [49]. Mn(IV) is expected to be less labile than Cr(III), but three O^{2-}, OH^- or $-COO^-$ groups per Mn site as spectator ligands may increase the water exchange for the ion in the WOC. A bridged μ-oxo is probably too inert to exchange in the range of 0.02–200 s^{-1}. However, two interconvertible structures could explain the spectroscopic properties of the WOC of PSII in the S_2 state [62]. Such interconvertible structures could help to increase water exchange (Fig. 11). This would be compatible with the mechanism suggested by Siegbahn for the S2 to S3 transition [63] that involves an additional H_2O binding at Mn1 of structure 1, but allows in principle for other possibilities if structure 2 also advances to S3 (Fig. 11). Pantazis et al. believe that the presence of an open coordination site along the Mn(III) pseudo Jahn–Teller axis is an inescapable result of the optimization of the photoreduced X-ray diffraction (XRD) structure and appears as a fundamental structural element of the S2-state (Fig. 11) [62].

Cox and Lubitz studied the hyperfine couplings of coordinating ^{17}O nuclei using W-band (94 GHz) electron–electron double resonance (ELDOR) to show three exchangeable O in the WOC during 15 s: one μ-oxo bridge, a terminal Mn–OH/OH_2 ligand, and Mn/Ca–H_2O ligand(s). In other words, they showed that one of the μ-oxo bridges and, at least, one of the two terminal water ligands of Mn(4) contributed to the measured ^{17}O-EDNMR (ELDOR-detected NMR) signal as seen using W-band EPR spectroscopy. The observation that a μ-oxo can exchange on this time scale is very interesting [64]. In 2013, Siegbahn studied water exchange in the S_1, S_2, and S_3 states using density functional theory (DFT) methods [63]. He suggested that water exchange at a reasonable rate for the WOC occurs with a water molecule bound to an Mn(III) site. The calculations show that Mn(3) has to be reduced to an Mn(III) state to release the bond to the substrate oxygen [63,65]. In other words, the mechanism of water exchange is more complicated than previously assumed [66].

The new mechanism of water exchange in S_1 is limited by a hydroxide exchange on the Mn(3) in a Mn(III) oxidation state. The calculations show that the high energy barrier of 21.7 kcal/mol is due to both an unfavorable electron transfer from Mn(4) to Mn(3), and a costly change of Jahn–Teller axis required for the hydroxide exchange (Fig. 12a).

Water exchange in S_2 may occur through a similar mechanism, but here the electron transfer from Mn(1) to create a Mn(III) state for Mn(3) occurs via a proton-coupled electron transfer (PCET) process, which has a lower rate limiting barrier of 17.6 kcal/mol. Siegbahn stated that it is not certain that the correct mechanism has been found but other mechanisms involving much higher barriers cannot be right (Fig. 12b).

Very recently, to assign the two substrate water sites of the WOC, pulsed EPR spectroscopy was used to demonstrate that one of the five oxygen bridges (μ-oxo) exchanges unusually rapidly with bulk water

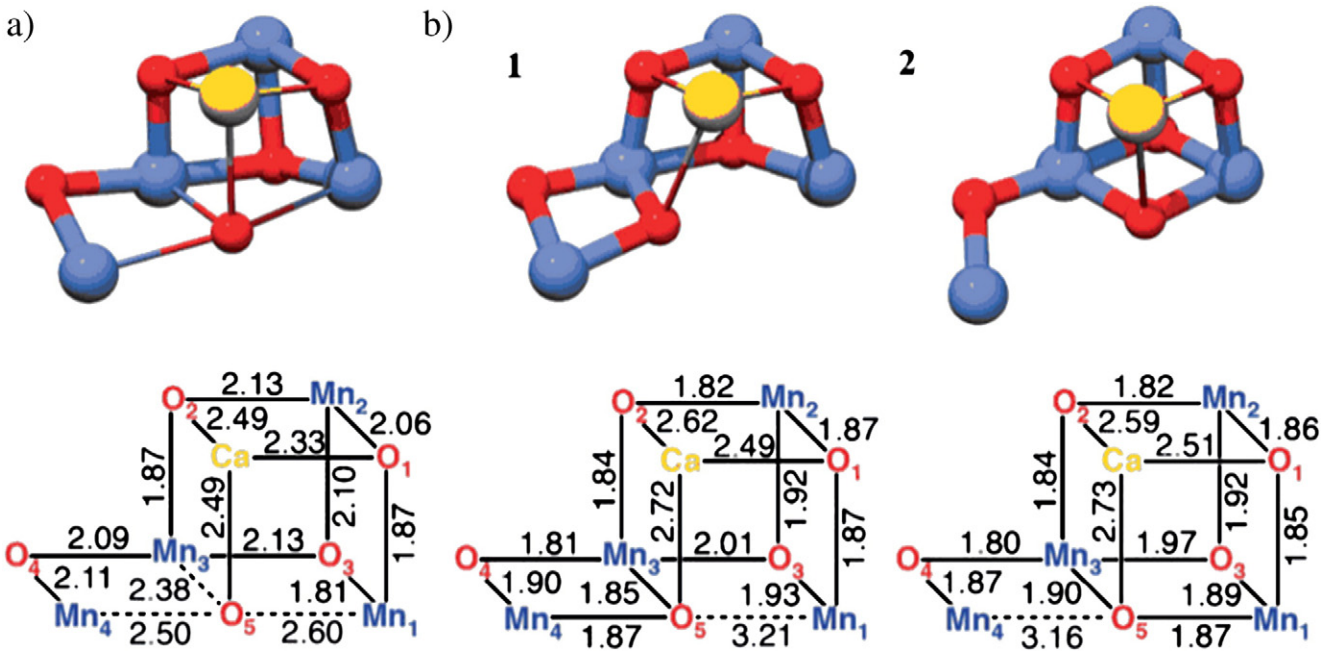

Fig. 11. Two interconvertible structures could explain the spectroscopic properties of the WOC of PSII in the S_2 state. Images are from [70].

and is thus a likely candidate for one of the substrates. Previous report by Britt shows that NH_3 binds to the Mn_4O_5Ca cluster [67]. In new experiments by W. Lubitz and N. Cox groups, a combination of EPR and time-resolved MIMS shows that the binding of ammonia perturbs the exchangeable μ-oxo bridge without drastically altering the binding/exchange kinetics of the two substrates [68]. These experiments in addition to broken-symmetry DFT show [68]:

i) O_5 is the exchangeable μ-oxo bridge (Fig. 9b)
ii) W1 (Fig. 9b) is displaced by ammonia, because of W1 is trans to O_5, ammonia binding elongates the Mn(4) – O_5 bond, leading to the perturbation of the μ-oxo bridge resonance and to a small change in the water exchange rates.
iii) Regarding Siegbahn's mechanism [69], O – O bond formation between O_5 and possibly an oxyl radical as proposed by and exclude W1 as the second substrate water.

This data constitutes of the first reports of highly exchangeable μ-O in the multinuclear Mn compounds. Mn compounds usually show slow water exchange for μ-O. Future details of water exchange for the WOC will be very important in understanding the mechanism of water oxidation in nature [48,66,70–80].

8. Mechanism of water oxidation by nano-layered Mn oxides: lessons from water exchange in a model compound

The synthesis and characterization of various Mn complexes aimed at simulating the WOC of PSII were reported by some groups [16,18–25,29,58,81–85]. These Mn complexes, besides modeling the WOC, would be highly desirable as key components for artificial photosynthesis — water splitting into H_2 and O_2, which is currently much discussed as a promising route for the conversion of solar, wind, ocean currents, tides or waves energy into hydrogen as "fuel" [16,18–25,29,58,81–85].

However, as shown by $H_2^{18}O$ isotope-labeling experiments coupled with membrane-inlet mass spectrometry (MIMS), few Mn complexes discovered so far are able to act as catalysts for real water oxidation [58,84]. However, Mn oxides, and most importantly nano-sized Mn oxides were reported as efficient catalysts for water oxidation.

Oxygen evolution by Mn oxides in $H_2^{18}O$ was studied in the presence of H_2O_2, hydrogen persulfate (HSO_5^-), cerium(IV) ammonium nitrate (Ce(IV)) and $[Ru^{III}(bpy)_3]^{3+}$ [85]. As Mn oxides are structural and functional models for the WOC in PSII [23,86], these studies are very interesting. Kurz and Messinger' groups used the method of MIMS [58] to detect the oxygen produced in reactions of Mn oxides in the presence of H_2O_2, HSO_5^-, Ce(IV) and $[Ru^{III}(bpy)_3]^{3+}$ in $H_2^{18}O$ [64]. In a MIMS, gas molecules from the sample solution pervaporate through a gas-permeable membrane into a magnetic sector field mass spectrometer. They detected clear signals for the O_2 isotopologues $^{16}O_2$ (m/z = 32), $^{16}O^{18}O$ (m/z = 34) and $^{18}O_2$ (m/z = 36) [85].

For these experiments, the fraction of ^{18}O atoms in the total O_2 produced was calculated according to $^{18}\alpha = ([^{18}O_2] + 0.5[^{16}O^{18}O])/[O_2]_{total}$. MIMS provides $[O_2]$ measurements and traces of the development of $^{18}\alpha$ over time could then be plotted for the course of the catalytic O_2-formation [85]. The incorporation of oxygen atoms from μ-O of the (Ca) Mn oxide into the released O_2 during the early stages of the reaction can be monitored with this method [85]. As reported by Kurz and Messinger' groups, the reaction of these Mn oxides with H_2O_2 or HSO_5^- is not water oxidation. In other words, the reaction of these Mn oxides with H_2O_2 constitutes a very fast oxygen evolution reaction but no incorporation of ^{18}O from the bulk water into the O_2 product was observed. On the other hand, the reaction of HSO_5^- with these Mn oxides produced oxygen at lower rates and in contrast with H_2O_2, $^{16}O^{18}O$ was detected [85].

The reaction of Ce(IV) or $[Ru^{III}(bpy)_3]^{3+}$, as single-electron, non-oxygen-transferring oxidants, is a real water reaction. The detection of oxygen in the reaction of $CaMn_2O_4 \cdot H_2O$ and Ce(IV) in water (5% $H_2^{18}O$) is shown in Fig. 13.

The $^{16}O_2$, $^{16}O^{18}O$ and $^{18}O_2$ species quickly rise after the addition of the oxidant and, in contrast to the H_2O_2 and HSO_5^-, the formation of $^{18}O_2$ is detected. $^{18}\alpha$ shows that the theoretically expected ^{18}O fraction of 5% is reached within only 30 s after the addition of Ce(IV) to the oxide suspension. These results show that the oxygen formed in reactions

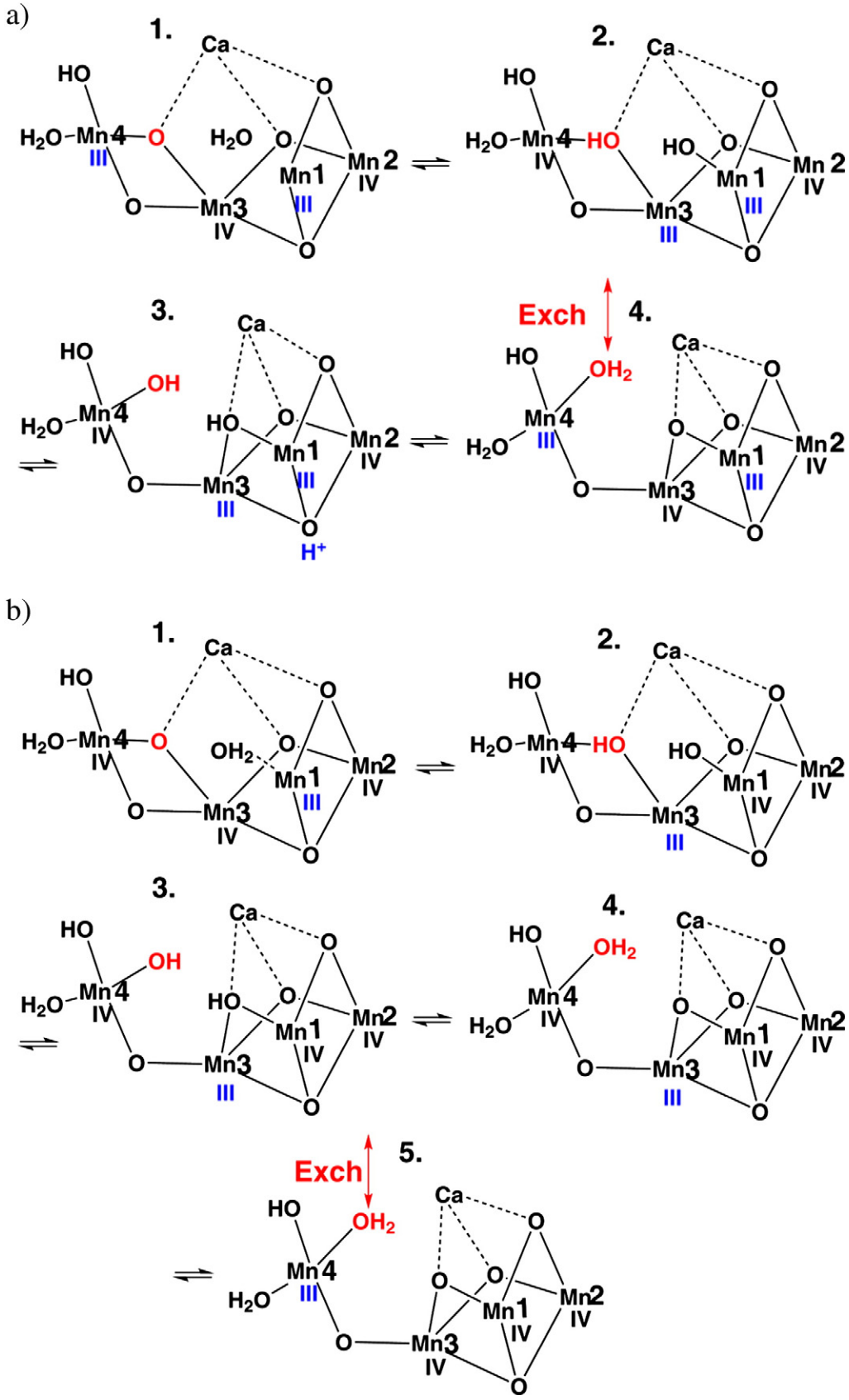

Fig. 12. Schematic mechanism for water exchange in the S_1 state of the WOC (a). Schematic mechanism for water exchange in the S_2 state of the WOC. The substrate oxygen is colored in red (b).
Image and caption from Ref. [71].

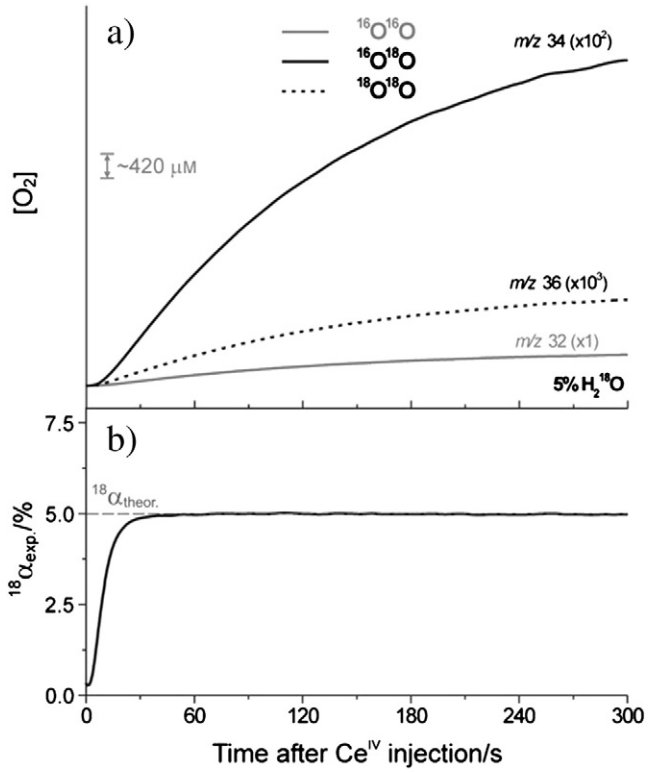

Fig. 13. (a) Oxygen evolution traces for the reaction of $CaMn_2O_4 \cdot H_2O$ with Ce(IV) detected by MIMS for $^{16}O_2$ (m/z = 32; solid gray trace), $^{16}O^{18}O$ (m/z = 34; solid black trace), and $^{18}O_2$ (m/z = 36; black dashed trace). A solution of Ce(IV) in $H_2^{18}O$ enriched water was injected into the (non-enriched) oxide suspension at t = 0 s. Final $CaMn_2O_4 \cdot H_2O$ and Ce(IV) in the MIMS cell were 1 mg·mL^{-1} and 100 mM, respectively. $H_2^{18}O$ enrichment of the reaction mixture: 5%. The pH of the medium was approximately 2. The absolute scale refers to an amplification factor of 1. (b) Change in A. The nano-sized layered Mn oxides show even more rate of water oxidation.
Image and caption are from Ref. [64].

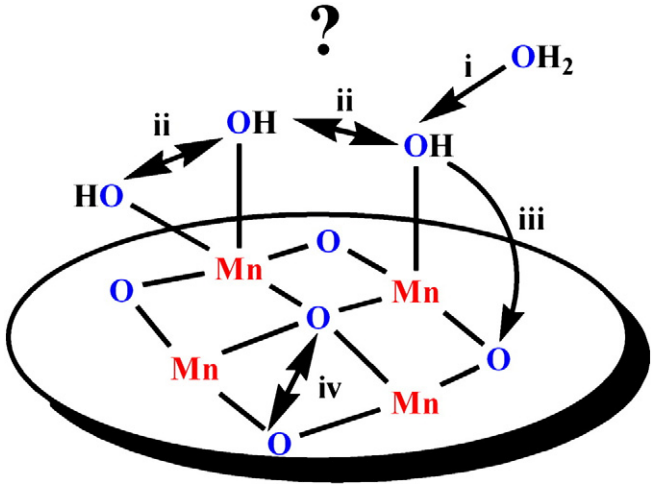

Fig. 14. Proposed mechanism of water oxidation by Mn oxides in the presence of Ce(IV). Red Mn ions show oxidized Mn ions. ^{16}O and ^{18}O are shown in pink and blue, respectively.

with Ce(IV) indeed originates from the oxidation of bulk water. The results in the presence of $[Ru^{III}(bpy)_3]^{3+}$ are similar to Ce(IV) but with slower oxygen evolution. From these experiments the group concluded as follows (routes a to c) [85]:

a) μ-O atoms on the surface are themselves not involved in the O – O bond formation (Fig. 14).
b) μ-O atoms on the surface are oxidized to form O_2 but also exchange with the bulk solution very rapidly.
c) The oxygen atoms of the oxide surface are involved in O – O bond formation, but the number of catalytic sites on the oxide surface is extremely small.

In addition, to find the possibility of reaction route c, the groups performed reactions in which a low concentration of Ce(IV) (6 mM) and a much higher ^{18}O–water labeling (50%) were used to observe the early stages of the oxygen evolution reaction that were not resolved in lower ^{18}O–water labeling experiments and this allowed the detection of the concentrations of $^{16}O^{18}O$ and $^{18}O_2$ for extended time periods without saturating the detector cups. From these experiments, they concluded that even in the early stages of the reaction of Ce(IV) with mes-terpy the possible incorporation of μ-O atoms on the surface is low (Fig. 15). Discrimination between routes a) or b) is not possible during these experiments. However, many of μ-O groups on the surface of Mn oxides are coordinated to three Mn ions and thus the water exchange is very slow for these μ-O.

From the results provided by several groups as discussed in previous sections, the time for water exchange of all μ-O is most probably longer than 30 s; thus if μ-O atoms on the surface are oxidized to form O_2, lower values are expected for $^{18}\alpha$ (Fig. 13a,b). Thus, the mechanism of water oxidation is most probably similar to the mechanism shown in Fig. 14.

Casey, Rustad, and Spiccia reviewed water exchange for aqueous oxide and hydroxide clusters [87]. They concluded that rates of water exchange bound to nanometer-sized oxides and most probably mineral surfaces, are robust and predictable by coupling experiments with rare-event simulation methods. They also proposed that the pathways for isotope exchanges at bridging oxygen atoms in nanometer-size clusters are extraordinarily counterintuitive. The proposed pathways appear to involve concerted motions of many ions to form a metastable structure that allows facile interaction with water (Fig. 16) [87].

Recently, Najafpour's groups used diffuse reflectance infrared Fourier transform spectroscopy to estimate the rate of $H_2^{18}O$ exchange for μ-O groups on the surface of nanolayered Mn–K oxide [89]. The results show that the rate of exchange for μ-O groups on the surface of the Mn–K oxide is too slow. These results in addition to results from previously reported MIMS provide new insights into mechanism of water oxidation by nanolayered Mn oxide [88]. The group proposed that the μ-O is not directly involved in O – O bond formation. O – O bond may be formed by (1) attack of an outer-sphere water to OH coordinated to high-valent Mn ion in oxide structure or (2) by the reaction between two OH that are coordinated to high-valent Mn ion(s). They have been observed two areas for water oxidation for Mn oxides: the first area for water oxidation that is near to the peak related to Mn(III)/Mn(IV) and another is 0.5 V higher than the first area. The group relates these points to pathways 2 and 1 in Fig. 14, respectively [88].

These results, in addition to results from previously reported membrane-inlet mass spectrometry, provide new insights into mechanism of water oxidation by nanolayered Mn oxide.

9. Conclusions

In conclusion, we reviewed the studies on water exchange for mono and multi-nuclear Mn compounds. Terminal water molecules usually exchange faster and bridged oxygen atoms very slowly. It is noted that terminal water ions help to improve the efficiency of bridged oxygen exchange. These data on water exchange and finding the ratio of $^{32}O_2$:$^{34}O_2$:$^{36}O_2$ in water oxidation are suggested to be very helpful to understand the mechanism of water oxidation in both artificial and natural systems.

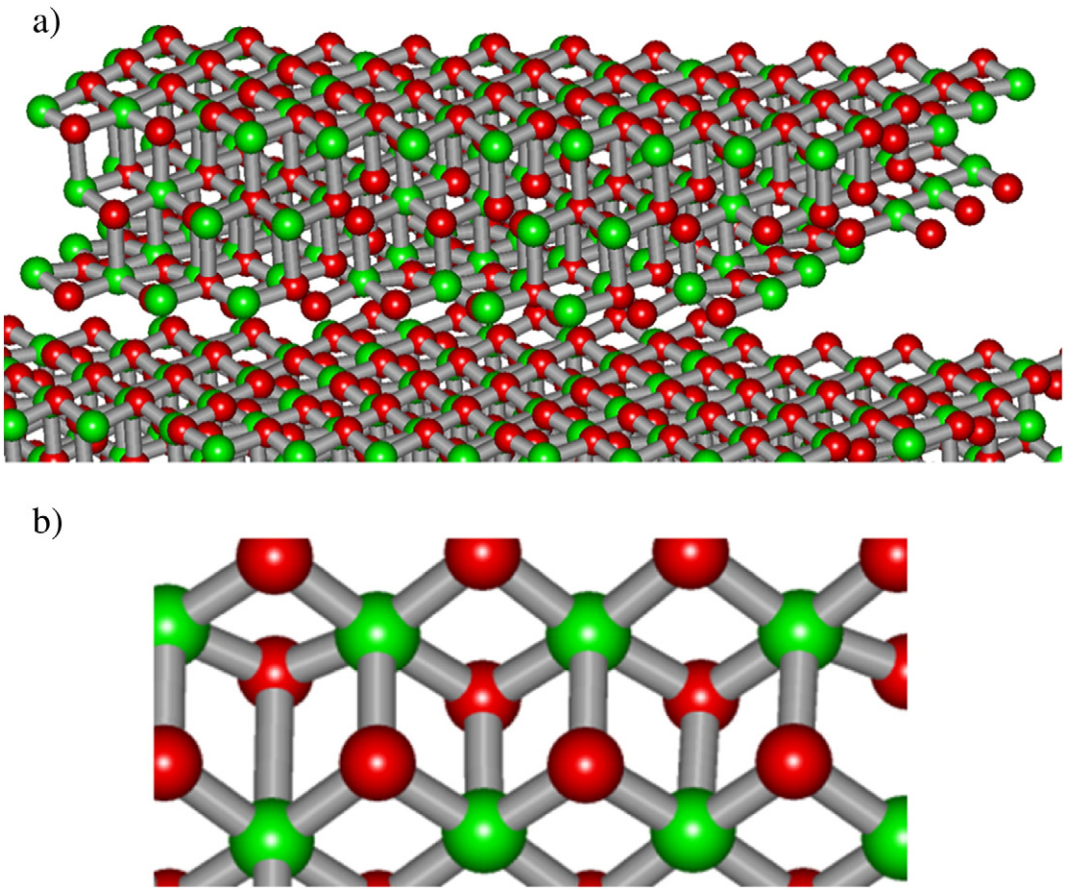

Fig. 15. A view of the surface of layered Mn oxide (red: O and Mn: green).

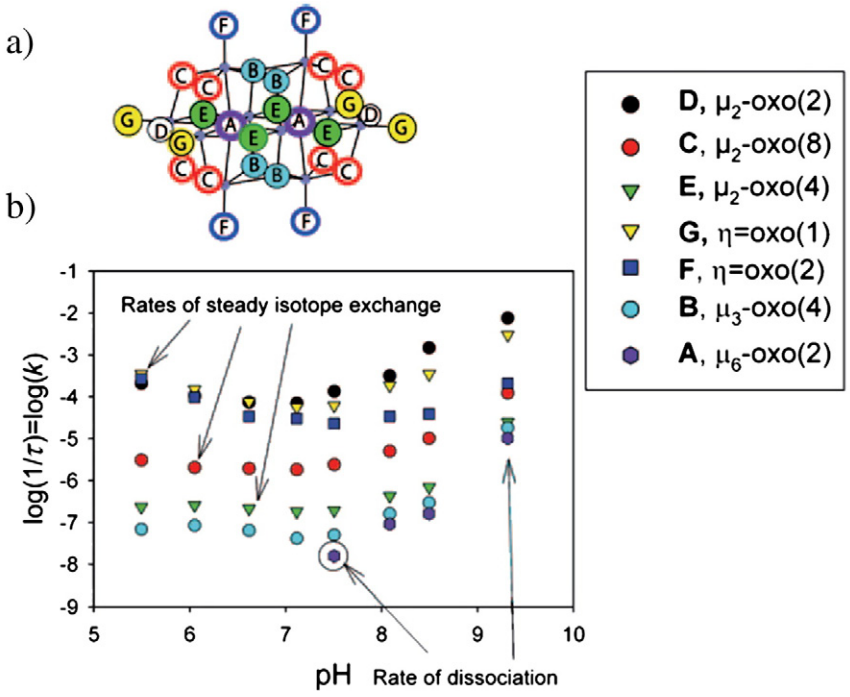

Fig. 16. All structural sites in a nanometer-size oxide ion respond to changes in solution pH. Here the rates of isotopic exchange and dissociation are shown for the decaniobate ion, which exhibit a profound pH dependence even at conditions under which the molecule is unprotonated. All oxygen atoms in this molecule respond to changes in solution composition. The rates of oxygen-isotope exchanges could be measured for the decaniobate ion at the seven oxygen sites (a). The ^{17}O NMR signal from the m6-oxo group changes with time only when the molecule begins to dissociate. Thus, the pH dependence of rates of steady oxygen isotope exchange can be compared to the rates of dissociation (b).
Image and caption are from [57].

Acknowledgements

MMN and MAI are grateful to the Institute for Advanced Studies in Basic Sciences and the National Elite Foundation for financial support. SIA was supported by grants from the Russian Foundation for Basic Research (Nos: 13-04-91372, 14-04-01549, 14-04-92102) by Molecular and Cell Biology Programs of the Russian Academy of Sciences. Authors thank professor Govindjee for his nice comments.

References

[1] T.J. Wydrzynski, K. Satoh, Photosystem II: The Light-Driven Water: Plastoquinone Oxidoreductase, Springer, Dordrecht, The Netherlands, 2005. 1–786.
[2] C. Eyster, Micronutrient requirements for green plants, especially algae, in: D.F. Jackson (Ed.), Algae and Man, Plenum Press, New York, 1961, pp. 86–119.
[3] A. Pirson, L. Bergmann, Manganese requirement and carbon source in *Chlorella*, Nature 176 (1955) 209–210.
[4] M.M. Najafpour, M.Z. Ghobadi, B. Haghighi, T. Tomo, R. Carpentier, J.-R. Shen, S.I. Allakhverdiev, A nano-sized manganese oxide in a protein matrix as a natural water-oxidizing site, Plant Physiol. Biochem. (2014), http://dx.doi.org/10.1016/j.plaphy.2014.01.020.
[5] N. Kamiya, J.-R. Shen, Crystal structure of oxygen-evolving photosystem II from *Thermosynechococcus vulcanus* at 3.7 Å resolution, Proc. Natl. Acad. Sci. U. S. A. 100 (2003) 98–103.
[6] A. Zouni, H.-T. Witt, J. Kern, P. Fromme, N. Krauss, W. Saenger, P. Orth, Crystal structure of photosystem II from *Synechococcus elongatus* at 3.8 Å resolution, Nature 409 (2001) 739–743.
[7] K.N. Ferreira, T.M. Iverson, K. Maghlaoui, J. Barber, S. Iwata, Architecture of the photosynthetic oxygen-evolving center, Science 303 (2004) 1831–1838.
[8] Y. Umena, K. Kawakami, J.-R. Shen, N. Kamiya, Crystal structure of oxygen-evolving photosystem II at a resolution of 1.9 Å, Nature 473 (2011) 55–60.
[9] D.J. Vinyard, G.M. Ananyev, G.C. Dismukes, Photosystem II: the reaction center of oxygenic photosynthesis, Annu. Rev. Biochem. 82 (2013) 577–606.
[10] J. Barber, P.D. Tran, From natural to artificial photosynthesis, J. R. Soc. Interface 10 (2013) 20120984.
[11] R. Pokhrel, G.W. Brudvig, Complex systems: photosynthesis, in: J. Reedijk, K. Poeppelmeier (Eds.), Second edition, Comprehensive Inorganic Chemistry II, vol. 3, Elsevier, Amsterdam, The Netherlands, 2013, pp. 385–422.
[12] P. Joliot, G. Barbieri, R. Chabaud, Un nouvean modele des centres photochimiques du systeme II, Photochem. Photobiol. 10 (1969) 309–329.
[13] B. Kok, B. Forbush, M. McGloin, Cooperation of charges in photosynthetic O_2 evolution. A linear four step mechanism, Photochem. Photobiol. 11 (1970) 457–475.
[14] P. Joliot, B. Kok, Oxygen evolution in photosynthesis, in: Govindjee (Ed.), Bioenergetics of Photosynthesis, Academic Press, New York, 1975, pp. 387–412.
[15] J. Messinger, G. Renger, Generation, oxidation by the oxidized form of the tyrosine of polypeptide D_2, and possible electronic configuration of the redox states S_0, S_{-1}, and S_{-2} of the water oxidase in isolated spinach thylakoids, Biochemistry 32 (1993) 9379–9386.
[16] C.W. Cady, R.H. Crabtree, G.W. Brudvig, Functional models for the oxygen-evolving complex of photosystem II, Coord. Chem. Rev. 252 (2008) 444–455.
[17] S.R. Cooper, M. Calvin, Mixed valence interactions in di-μ-oxo bridged manganese complexes, J. Am. Chem. Soc. 99 (1977) 6623–6630.
[18] M.M. Najafpour, Manganese compounds as water oxidizing catalysts in artificial photosynthesis, in: M.M. Najafpour (Ed.), Artificial Photosynthesis, Tech Publications, Rijeka, Croatia, 2012, pp. 37–52.
[19] M.M. Najafpour, Hollandite as a functional and structural model for the biological water oxidizing complex: manganese–calcium oxide minerals as a possible evolutionary origin for the $CaMn_4$ cluster of the biological water oxidizing complex, Geomicrobiol J. 28 (2011) 714–718.
[20] M.M. Najafpour, S.I. Allakhverdiev, Manganese compounds as water oxidizing catalysts for hydrogen production via water splitting: from manganese complexes to nano-sized manganese oxides, Int. J. Hydrogen Energy 37 (2012) 8753–8764.
[21] M.M. Najafpour, S. Nayeri, B. Pashaei, Nano-size amorphous calcium–manganese oxide as an efficient and biomimetic water oxidizing catalyst for artificial photosynthesis: back to manganese, Dalton Trans. 40 (2011) 9374–9378.
[22] M.M. Najafpour, B. Pashaei, S. Nayeri, Nano-sized layered aluminium or zinc–manganese oxides as efficient water oxidizing catalysts, Dalton Trans. 41 (2012) 7134–7140.
[23] M.M. Najafpour, F. Rahimi, E.-M. Aro, C.-H. Lee, S.I. Allakhverdiev, Nano-sized manganese oxides as biomimetic catalysts for water oxidation in artificial photosynthesis: a review, J. R. Soc. Interface 9 (2012) 2383–2395.
[24] M.M. Najafpour, D.J. Sedigh, Water oxidation by manganese oxides, a new step towards a complete picture: simplicity is the ultimate sophistication, Dalton Trans. 42 (2013) 12173–12178.
[25] M.M. Najafpour, D.J. Sedigh, B. Pashaei, S. Nayeri, Water oxidation by nano-layered manganese oxides in the presence of cerium(IV) ammonium nitrate: important factors and a proposed self-repair mechanism, New J. Chem. 37 (2013) 2448–2459.
[26] W. Ruttinger, G.C. Dismukes, Synthetic water-oxidation catalysts for artificial photosynthetic water oxidation, Chem. Rev. 97 (1997) 1–24.
[27] A. Singh, L. Spiccia, Water oxidation catalysts based on abundant 1st row transition metals, Coord. Chem. Rev. 257 (2013) 2607–2622.
[28] R. Tagore, R.H. Crabtree, G.W. Brudvig, Oxygen evolution catalysis by a dimanganese complex and its relation to photosynthetic water oxidation, Inorg. Chem. 47 (2008) 1815–1823.
[29] H.J.M. Hou, Structural and mechanistic aspects of Mn-oxo and Co-based compounds in water oxidation catalysis and potential applications in solar fuel production, J. Integr. Plant Biol. 52 (2013) 704–711.
[30] R. Brimblecombe, A. Koo, G.C. Dismukes, G.F. Swiegers, L. Spiccia, Solar driven water oxidation by a bioinspired manganese molecular catalyst, J. Am. Chem. Soc. 132 (2010) 2892–2894.
[31] R.K. Hocking, R. Brimblecombe, L.-Y. Chang, A. Singh, M.H. Cheah, C. Glover, W.H. Casey, L. Spiccia, Water-oxidation catalysis by manganese in a geochemical-like cycle, Nat. Chem. 3 (2011) 461–466.
[32] Metals in biology, in: G.R. Hanson, L.J. Berliner (Eds.), Biological Magnetic Resonance, Springer, New York, 2010.
[33] W. Hillier, T. Wydrzynski, ^{18}O–water exchange in photosystem II: substrate binding and intermediates of the water splitting cycle, Coord. Chem. Rev. 252 (2008) 306–317.
[34] L. Helm, A.E. Merbach, Inorganic and bioinorganic solvent exchange mechanisms, Chem. Rev. 105 (2005) 1923–1960.
[35] R.G. Wilkins, The Study of Kinetics and Mechanism of Reactions of Transition Metal Complexes, Allyn and Bacon, Boston, 1974. 1–183.
[36] N.S. Imyanitov, Is this reaction a substitution, oxidation–reduction, or transfer? J. Chem. Educ. 70 (1993) 14–16.
[37] Advanced Organic Chemistry: Reactions, Mechanisms, and Structure, in: J. March (Ed.), John Wiley & Sons, New York, 1992, pp. 1–1512.
[38] C.H. Langford, H.B. Gray, Ligand substitution processes, in: R. Breslaw, N. Karplus (Eds.), Frontiers in Chemistry, Benjamin, W.A. Inc., New York, 1966, pp. 33–111.
[39] A.L. Petrou, M. Economou-Eliopoulos, Platinum-group mineral formation: evidence of an interchange process from the entropy of activation values, Geochim. Cosmochim. Acta Ac73 (2009) 5635–5645.
[40] J.V. Quagliano, L.E.O. Schubert, The trans effect in complex inorganic compounds, Chem. Rev. 50 (1952) 201–260.
[41] H. Diebler, N. Sutin, The kinetics of some oxidation–reduction reactions involving manganese(III), J. Phys. Chem. 68 (1964) 174–180.
[42] T. Takashima, K. Hashimoto, R. Nakamura, Inhibition of charge disproportionation of MnO_2 electrocatalysts for efficient water oxidation under neutral conditions, J. Am. Chem. Soc. 134 (2012) 18153–18156.
[43] D. Lieb, A. Zahl, T.E. Shubina, I. Ivanovicl̀-Burmazovicl̀, Water exchange on manganese (III) porphyrins. Mechanistic insights relevant for oxygen evolving complex and superoxide dismutation catalysis, J. Am. Chem. Soc. 132 (2010) 7282–7284.
[44] E. Balogh, Z. He, W. Hsieh, S. Liu, E. Toth, Dinuclear complexes formed with the triazacyclononane derivative $ENOTA^{4-}$: high-pressure ^{17}O NMR evidence of an associative water exchange on $[Mn^{II}_2(ENOTA)(H_2O)_2]$, Inorg. Chem. 46 (2007) 238–250.
[45] A. Dees, A. Zahl, R. Puchta, N.J.R. van Eikema Hommes, F.W. Heinemann, I. Ivanovic-Burmazovic, Water exchange on seven-coordinate Mn(II) complexes with macrocyclic pentadentate ligands: insight in the mechanism of Mn(II) SOD mimetics, Inorg. Chem. 46 (2007) 2459–2470.
[46] J. Maigut, R. Meier, A. Zahl, R.v. Eldik, Triggering water exchange mechanisms via chelate architecture. Shielding of transition metal centers by aminopolycarboxylate spectator ligands, J. Am. Chem. Soc. 130 (2008) 14556–14569.
[47] T. Schneppensieper, A. Zahl, R. van Eldik, Water exchange controls the complex-formation mechanism of water-soluble iron(III) porphyrins: conclusive evidence for dissociative water exchange from a high-pressure ^{17}O NMR study, Angew. Chem. Int. Ed. 40 (2001) 1678–1680.
[48] J.R. Houston, P. Yu, W.H. Casey, Water exchange from the oxo-centered rhodium(III) trimer $[Rh_3(\mu\text{-}O)(\mu\text{-}O_2CCH_3)_6(OH_2)]^{3+}$: a high-pressure ^{17}O NMR study, Inorg. Chem. 44 (2005) 5176–5182.
[49] S.J. Crimp, L. Spiccia, H.R. Krouse, T.W. Swaddle, Swaddle, early stages of the hydrolysis of chromium(III) in aqueous solution. Kinetics of water exchange on the hydrolytic dimer, Inorg. Chem. 33 (1994) 465–470.
[50] K.R. Rodgers, R.K. Murmann, E.O. Schlemper, M.E. Shelton, Rates of isotopic oxygen exchange with solvent and oxygen atom transfer involving nonaaquatetraoxotrimolybdenum $((4+)([Mo_3O_4(OH_2)_9])^{4+})$, Inorg. Chem. 24 (1985) 1313–1322.
[51] A. Drljaca, A. Zahl, R. van Eldik, High-pressure ^{17}O NMR study of the dihydroxo-bridged rhodium(III) hydrolytic dimer. Mechanistic evidence for limiting dissociative water exchange pathways, Inorg. Chem. 37 (1998) 3948–3953.
[52] R. Tagore, H. Chen, R.H. Crabtree, G.W. Brudvig, Determination of μ-oxo exchange rates in di-μ-oxo dimanganese complexes by electrospray ionization mass spectrometry, J. Am. Chem. Soc. 128 (2006) 9457–9465.
[53] W.H. Casey, B.L. Phillips, M. Karlsson, S. Nordin, J.P. Nordin, D.J. Sullivan, S. Neugebauer-Crawford, Rates and mechanisms of oxygen exchanges between sites in the $AlO_4Al_{12}(OH)_{24}(H_2O)^{7+}_{12}(aq)$ complex and water: implications for mineral surface chemistry, Geochim. Cosmochim. Acta 64 (2000) 2951–2964.
[54] J.R. Rustad, J.S. Loring, W.H. Casey, Oxygen-exchange pathways in aluminum polyoxocations, Geochim. Cosmochim. Acta 68 (2004) 3011–3017.
[55] I.L. McConnell, V.M. Grigoryants, C.P. Scholes, W.K. Myers, P.-Y. Chen, J.W. Whittaker, G.W. Brudvig, EPR-ENDOR characterization of (^{17}O, ^{1}H, ^{2}H) water in manganese catalase and its relevance to the oxygen-evolving complex of photosystem II, J. Am. Chem. Soc. 134 (2012) 1504–1512.
[56] C.A. Ohlin, R. Brimblecombe, L. Spiccia, W.H. Casey, Oxygen isotopic exchange in an $Mn^{III}Mn^{IV}_3$-oxo cubane, Dalton Trans. (2009) 5278–5280.
[57] J.S. Kanady, J.L. Mendoza-Cortes, E.Y. Tsui, R.J. Nielsen, W.A. Goddard Iii, T. Agapie, Oxygen atom transfer and oxidative water incorporation in cuboidal Mn_3MO n complexes based on synthetic, isotopic labeling, and computational studies, J. Am. Chem. Soc. 135 (2013) 1073–1082.

[58] K. Beckmann, J. Messinger, M.R. Badger, T. Wydrzynski, W. Hillier, On-line mass spectrometry: membrane inlet sampling, Photosynth. Res. 102 (2009) 511–522.
[59] A. Bergmann, I. Zaharieva, H. Dau, P. Strassera, Energy Environ. Sci. 6 (2013) 2745–2755.
[60] N. Birkner, S. Nayeri, B. Pashaei, M.M. Najafpour, W.H. Casey, A. Navrotsky, Energetic basis of catalytic activity of layered nanophase calcium manganese oxides for water oxidation, Proc. Natl. Acad. Sci. U. S. A. 110 (2013) 8801–8806.
[61] F. Jiao, H. Frei, Nanostructured manganese oxide clusters supported on mesoporous silica as efficient oxygen-evolving catalysts, Chem. Commun. 46 (2011) 2920–2922.
[62] E.A. Karlsson, B.L. Lee, T. Åkermark, E.V. Johnston, M.D. Kärkäs, J. Sun, Ö. Hansson, J.E. Bäckvall, B. Åkermark, Photosensitized water oxidation by use of a bioinspired manganese catalyst, Angew. Chem. Int. Ed. 123 (2011) 11919–11922.
[63] M. Yagi, M. Kaneko, Molecular catalysts for water oxidation, Chem. Rev. 101 (2001) 21–36.
[64] D. Shevela, S. Koroidov, M.M. Najafpour, J. Messinger, P. Kurz, Calcium manganese oxides as oxygen evolution catalysts: O_2 formation pathways indicated by ^{18}O-labelling studies, Chem. Eur. J. 17 (2011) 5415–5423.
[65] M.M. Najafpour, A.N. Moghaddam, Y.N. Yang, E.-M. Aro, R. Carpentier, J.J. Eaton-Rye, C.-H. Lee, S.I. Allakhverdiev, Biological water-oxidizing complex: a nano-sized manganese calcium oxide in a protein environment, Photosynth. Res. 114 (2012) 1–13.
[66] W.H. Casey, J.R. Rustad, L. Spiccia, Minerals as molecules — use of aqueous oxide and hydroxide clusters to understand geochemical reactions, Chem. Eur. J. 15 (2009) 4496–4515.
[67] L. Konermann, J. Messinger, W. Hillier, Mass spectrometry-based methods for studying kinetics and dynamics in biological systems, in: T.J. Aartsma, J. Matysik (Eds.), Biophysical Techniques in Photosynthesis, Springer, Dordrecht, The Netherlans, 2008, pp. 167–190.
[68] N. Cox, J. Messinger, Reflections on substrate water and dioxygen formation, Biochim. Biophys. Acta 1827 (2013) 1020–1030.
[69] J. Lavergne, W. Junge, Proton release during the redox cycle of the water oxidase, Photosynth. Res. 38 (1993) 279–296.
[70] D.A. Pantazis, W. Ames, N. Cox, W. Lubitz, F. Neese, Two interconvertible structures that explain the spectroscopic properties of the oxygen-evolving complex of photosystem ii in the S_2 state, Angew. Chem. Int. Ed. 51 (2012) 9935–9940.
[71] P.E.M. Siegbahn, Substrate water exchange for the oxygen evolving complex in PSII in the S_1, S_2 and S_3 states, J. Am. Chem. Soc. 135 (2013) 9442–9449.
[72] L. Rapatskiy, N. Cox, A. Savitsky, W.M. Ames, J. Sander, M.M. Nowaczyk, M. Rol̂gner, A. Boussac, F. Neese, J. Messinger, Detection of the water-binding sites of the oxygen-evolving complex of photosystem II using W-band ^{17}O electron–electron double resonance-detected NMR spectroscopy, J. Am. Chem. Soc. 134 (2012) 16619–16634.
[73] Primary Processes of Photosynthesis: Principles and Apparatus, in: G. Renger (Ed.), Royal Society of Chemistry, Cambridge, 2008, pp. 1–496.
[74] P.E.M. Siegbahn, Mechanisms for proton release during water oxidation in the S_2 to S_3 and S_3 to S_4 transitions in photosystem II, Phys. Chem. Chem. Phys. 14 (2012) 4849–4856.
[75] R.D. Britt, J.L. Zimmermann, K. Sauer, M.P. Klein, Ammonia binds to the catalytic manganese of the oxygen-evolving complex of photosystem II. Evidence by electron spin-echo envelope modulation spectroscopy, J. Am. Chem. Soc. 111 (1989) 3522–3532.
[76] M.P. Navarro, W.M. Ames, H.k. Nilsson, T. Lohmiller, D.A. Pantazis, L. Rapatskiy, M.M. Nowaczyk, F. Neese, A. Boussac, J. Messinger, Ammonia binding to the oxygen-evolving complex of photosystem II identifies the solvent-exchangeable oxygen bridge (μ-oxo) of the manganese tetramer, Proc. Natl. Acad. Sci. U. S. A. 110 (2013) 15561–15566.
[77] R.D. Britt, K.A. Campbell, J.M. Peloquin, M.L. Gilchrist, C.P. Aznar, M.M. Dicus, J. Robblee, J. Messinger, Recent pulsed EPR studies of the photosystem II oxygen-evolving complex: implications as to water oxidation mechanisms, Biochim. Biophys. Acta 1655 (2004) 158–171.
[78] G.W. Brudvig, Water oxidation chemistry of photosystem II, Philos. Trans. R. Soc. Lond. B 363 (2008) 1211–1219.
[79] H.-A. Chu, Fourier transform infrared difference spectroscopy for studying the molecular mechanism of photosynthetic water oxidation, Front. Plant Sci. (2010), http://dx.doi.org/10.3389/fpls.2013.00146.
[80] A. Galstyan, A. Robertazzi, E.W. Knapp, Oxygen-evolving Mn cluster in photosystem II: the protonation pattern and oxidation state in the high-resolution crystal structure, J. Am. Chem. Soc. 134 (2012) 7442–7449.
[81] A. Grundmeier, H. Dau, Structural models of the manganese complex of photosystem II and mechanistic implications, Biochim. Biophys. Acta 1817 (2012) 88–105.
[82] C.W. Hoganson, G.T. Babcock, A metalloradical mechanism for the generation of oxygen from water in photosynthesis, Science 277 (1997) 1953–1956.
[83] N. Ioannidis, J.H.A. Nugent, V. Petrouleas, Intermediates of the S3 state of the oxygen-evolving complex of photosystem II, Biochemistry 41 (2002) 9589–9600.
[84] J. Limburg, V.A. Szalai, G.W. Brudvig, A mechanistic and structural model for the formation and reactivity of a MnV═O species in photosynthetic water oxidation, J. Chem. Soc. Dalton Trans. (1999) 1353–1362.
[85] V.L. Pecoraro, M.J. Baldwin, M.T. Caudle, W.-Y. Hsieh, N.A. Law, A proposal for water oxidation in photosystem II, Pure Appl. Chem. 70 (1998) 925–930.
[86] P.E.M. Siegbahn, Water oxidation mechanism in photosystem II, including oxidations, proton release pathways: O – O bond formation and O_2 release, Biochim. Biophys. Acta 1827 (2014) 1003–1019.
[87] E.M. Sproviero, J.A. Gascon, J.P. McEvoy, G.W. Brudvig, V.S. Batista, A model of the oxygen-evolving center of photosystem II predicted by structural refinement based on EXAFS simulations, J. Am. Chem. Soc. 130 (2008) 6728–6730.
[88] H. Suzuki, M. Sugiura, T. Noguchi, Monitoring water reactions during the S-state cycle of the photosynthetic water-oxidizing center: detection of the DOD bending vibrations by means of Fourier transform infrared spectroscopy, Biochemistry 47 (2008) 11024–11030.
[89] M.M. Najafpour, M. Abbasi Isaloo, Mechanism of water oxidation by nanolayered manganese oxide: a step forward, RSC Adv. 4 (2014) 6375–6378.